



GMNIA with beam elements and strain limits based fire design approach for steel beams and beam–columns

Hasan Murtaza, Merih Kucukler*

School of Engineering, University of Warwick, Coventry, CV4 7AL, UK

ARTICLE INFO

Keywords:

Anisothermal analysis
Continuous Strength Method (CSM)
CSM strain limits
Fire design
GMNIA
Isothermal analysis
Local buckling

ABSTRACT

The use of advanced analysis techniques harnessing the capabilities of the currently available computational resources can lead to considerably more accurate fire design of steel structures relative to the currently adopted simple fire design methods in practice. In this paper, a structural steel fire design method by Geometrically and Materially Nonlinear Analysis with Imperfections (GMNIA) and using strain limits is put forward for the fire design of steel beams and beam–columns. In the proposed fire design method, the GMNIA of a steel member or structure is performed using computationally efficient beam finite elements and strain limits are adopted to account for the detrimental effects of local buckling on the ultimate capacities. To verify the accuracy of the proposed method, extensive numerical parametric studies are conducted through shell finite element modelling. The results indicate that the proposed approach provides accurate and safe ultimate resistance and limit temperature estimations for steel beams and beam–columns in fire, with a considerably higher level of accuracy and reliability relative to the provisions of the European structural steel fire design standard EN 1993-1-2.

1. Introduction

In fire, steel structures exhibit complex structural response, which has to be adequately accounted for in their fire design. However, despite their sophisticated behaviour at elevated temperatures, currently, the fire design of steel structures is generally carried out by means of simple design methods provided in structural steel fire design standards. These simple structural steel fire design methods which can be applied through hand calculations are based on a high number of simplifications and assumptions, leading to the inaccurate assessment of the behaviour of steel structures in fire in some cases. Given the development of sophisticated numerical analysis techniques [1–5] together with the wide availability of computers and finite element analysis software in recent years, an advanced structural steel fire design framework able to utilise the current computational resources available to structural engineers in practice can much more accurately capture the complex structural response of steel structures in fire. The research presented in this paper is directed towards this objective, aiming to establish a new structural steel fire design approach that effectively uses the computational resources currently available to the structural engineering profession.

At elevated temperatures, (i) the strength and stiffness of steel significantly deteriorate, (ii) the material behaviour becomes considerably nonlinear, (iii) thermal expansions occur and (iv) indirect fire

actions (i.e. indirect internal forces) develop within steel elements due to the restrictions to thermal expansions; these detrimental factors can significantly reduce the ultimate resistances of steel structures in fire. The current version of the European structural steel fire design standard EN 1993-1-2 [6] as well as its next revision prEN 1993-1-2 [7] provide two types of design models to account for the detrimental factors in the fire design of steel structures, which are referred to as (i) the simple calculation models and (ii) the advanced calculation models; though for the advanced calculation models, the guidelines in [6,7] are quite limited. The simple calculation models of EN 1993-1-2 [6] are simple extensions of room temperature structural steel design methods and they are significantly more widely used for the fire design of steel structures in practice. On the other hand, the advanced calculation models recommended in EN 1993-1-2 [6] and prEN 1993-1-2 [7] require performing nonlinear finite element analyses of steel structures in fire, which can typically be carried out by means of beam finite elements in practice due to their computational efficiency. Both simple calculation models and advanced calculation models implemented employing beam finite elements require the use of the cross-section classification and effective width methods for the consideration of the local instability effects on the behaviour of steel elements at elevated temperatures. However, this approach for the consideration of local buckling effects in structural steel members in fire has a number of

* Corresponding author.

E-mail addresses: hasan.murtaza@warwick.ac.uk (H. Murtaza), merih.kucukler@warwick.ac.uk (M. Kucukler).

significant shortcomings in that it (i) disregards the continuity between the cross-section resistance and cross-section slenderness, (ii) ignores the cross-section element interactions during local buckling, (iii) does not take into account the development of partial plasticity particularly within Class 3 (semi-compact) as well as in some Class 4 (slender) sections and (iv) has been shown to provide somewhat inaccurate predictions of the ultimate capacities of steel cross-sections at elevated temperatures [8–12].

For the purpose of establishing a structural steel fire design method able to provide accurate estimations of the structural response of steel structures at elevated temperatures, Murtaza and Kucukler [13] recently (i) put forward a new structural steel fire design approach through Geometrically and Materially Nonlinear Analysis with Imperfections (GMNIA) and strain limits and (ii) applied it to the fire design of steel columns, extending the room temperature structural steel design approach using GMNIA with strain limits developed in [14–19] to structural steel fire design. In this paper, the fire design method by GMNIA with strain limits introduced in [13] is extended to the fire design of steel beams and beam–columns as part of the establishment of a novel fire design framework for steel structures. In the proposed structural steel fire design method, the second-order inelastic analysis or Geometrically and Materially Nonlinear Analysis with Imperfections (GMNIA) of a steel member or structure in fire is carried out by means of computationally efficient beam finite elements, and strain limits calculated using a modified continuous strength method (CSM) base curve are used to consider local instability effects. The ultimate capacity of a steel member or structure is determined as (i) the load or temperature level at which the predefined strain limit is attained or (ii) the peak load or critical temperature observed during the analysis, whichever occurs first. The proposed structural steel fire design approach removes the requirements for separate member and cross-section design checks, resulting in a principally self-contained fire design method where (i) the deteriorations in material strengths and stiffnesses in fire, (ii) thermal expansions, (iii) indirect fire actions resulting from restrictions to thermal expansions, (iv) geometric and material nonlinearities, (v) member instabilities and (vi) failure modes of steel structures in fire are explicitly captured during the analysis. Due to the inability of conventional beam finite elements to capture the detrimental influence of local buckling on resistance, in the proposed fire design approach, local buckling is considered through imposing predefined strain limits on steel members in fire which are determined on the basis of the cross-section slenderness, thereby (i) accounting for cross-section element interactions during local buckling and (ii) establishing a continuous relationship between cross-section deformation capacity and cross-section slenderness.

In the following sections of this paper, concepts related to the fire design of steel beams and beam–columns using the proposed structural steel fire approach are introduced. Benchmark shell finite element models capable of replicating the behaviour of steel beams and beam–columns at elevated temperatures are developed and validated against experimental results from the literature. The ultimate capacities of steel beams and beam–columns determined through the proposed structural steel fire design approach are compared against those obtained from the developed shell finite element models as well as those determined through EN 1993-1-2 [6] provisions. The results indicate that the proposed method provides significantly more accurate and safe-sided capacity predictions for steel beams and beam–columns at elevated temperatures relative to EN 1993-1-2 [6]. It should be noted that in this study, the structural response and design of steel I-section beams and beam–columns not susceptible to flexural–torsional buckling are taken into consideration. The proposed fire design approach will be extended to the flexural–torsional buckling assessment of steel I-section beams and beam–columns at elevated temperatures as well as to the fire design of steel frames in future research.

2. Fire design by GMNIA with strain limits

This section describes the primary principles of the proposed fire design method by GMNIA with strain limits.

2.1. Fundamentals of proposed method

The proposed structural steel fire design approach is essentially based on (i) the GMNIA of a structure in fire performed using beam finite elements and (ii) a base curve which relates the elevated temperature cross-section deformation capacity to the elevated temperature cross-section slenderness; using the latter, compressive strain limits are determined for structural steel members at elevated temperatures and used to take into consideration the detrimental effects of local buckling on resistance in fire.

The proposed method can be applied adopting either (i) the isothermal (i.e. steady-state) analysis technique where the temperature of a steel element is initially increased and then it is loaded up to failure or (ii) the anisothermal (i.e. transient) analysis technique where a steel element is loaded first and then heated up to failure.

2.2. Material model

The proposed fire design method by GMNIA with strain limits adopts the EN 1993-1-2 [6] elevated temperature material model shown in Fig. 1 and formulated in Eq. (1)

$$\sigma = \begin{cases} \epsilon E_{\theta} & \text{for } \epsilon \leq \epsilon_{p,\theta} \\ f_{p,\theta} - c + (b/a)\sqrt{a^2 - (\epsilon_{2,\theta} - \epsilon)^2} & \text{for } \epsilon_{p,\theta} < \epsilon < \epsilon_{2,\theta} \\ f_{2,\theta} & \text{for } \epsilon_{2,\theta} < \epsilon < \epsilon_{t,\theta} \\ f_{2,\theta}[1 - (\epsilon - \epsilon_{t,\theta})/(\epsilon_{u,\theta} - \epsilon_{t,\theta})] & \text{for } \epsilon_{t,\theta} < \epsilon < \epsilon_{u,\theta} \\ 0 & \text{for } \epsilon = \epsilon_{u,\theta} \end{cases} \quad (1)$$

where σ and ϵ are the stress and strain, E_{θ} is the elevated temperature Young's modulus, $f_{p,\theta}$ is the elevated temperature proportional limit stress, $f_{2,\theta}$ is the elevated temperature material strength at 2% total strain, $\epsilon_{p,\theta}$ is the strain value at the proportional limit calculated as $\epsilon_{p,\theta} = f_{p,\theta}/E_{\theta}$, $\epsilon_{2,\theta}$ is the 2% total strain (i.e. $\epsilon_{2,\theta} = 0.02$), $\epsilon_{t,\theta}$ is the limit strain equal to 0.15 (i.e. $\epsilon_{t,\theta} = 0.15$) and $\epsilon_{u,\theta}$ is the ultimate strain taken as 0.20 (i.e. $\epsilon_{u,\theta} = 0.20$). Note that the elevated temperature material properties are determined by multiplying the room temperature material properties such as the Young's modulus E and yield strength f_y by the corresponding Young's modulus reduction factor $k_{E,\theta}$, the proportional limit stress reduction factor $k_{p,\theta}$ and the yield strength reduction factor $k_{y,\theta}$ given by EN 1993-1-2 [6] and displayed in Fig. 1(b). Additionally, the coefficients a , b and c used in Eq. (1) are calculated as given below in accordance with EN 1993-1-2 [6]:

$$\begin{aligned} a &= \sqrt{(\epsilon_{2,\theta} - \epsilon_{p,\theta})(\epsilon_{2,\theta} - \epsilon_{p,\theta} + c/E_{\theta})}, \\ b &= \sqrt{c(\epsilon_{2,\theta} - \epsilon_{p,\theta})E_{\theta} + c^2}, \\ c &= \frac{(f_{2,\theta} - f_{p,\theta})^2}{(\epsilon_{2,\theta} - \epsilon_{p,\theta})E_{\theta} - 2(f_{2,\theta} - f_{p,\theta})}. \end{aligned} \quad (2)$$

2.3. Cross-section slenderness

In the implementation of the proposed fire design method, the calculation of the elevated temperature cross-section slendernesses $\bar{\lambda}_{p,\theta}$ of structural steel members is necessary. The elevated temperature cross-section slenderness $\bar{\lambda}_{p,\theta}$ of a steel member can be calculated as

$$\bar{\lambda}_{p,\theta} = \bar{\lambda}_p \sqrt{\frac{k_{p0,2,\theta}}{k_{E,\theta}}} = \sqrt{\frac{f_y}{\sigma_{cr,cs}}} \sqrt{\frac{k_{p0,2,\theta}}{k_{E,\theta}}}, \quad (3)$$

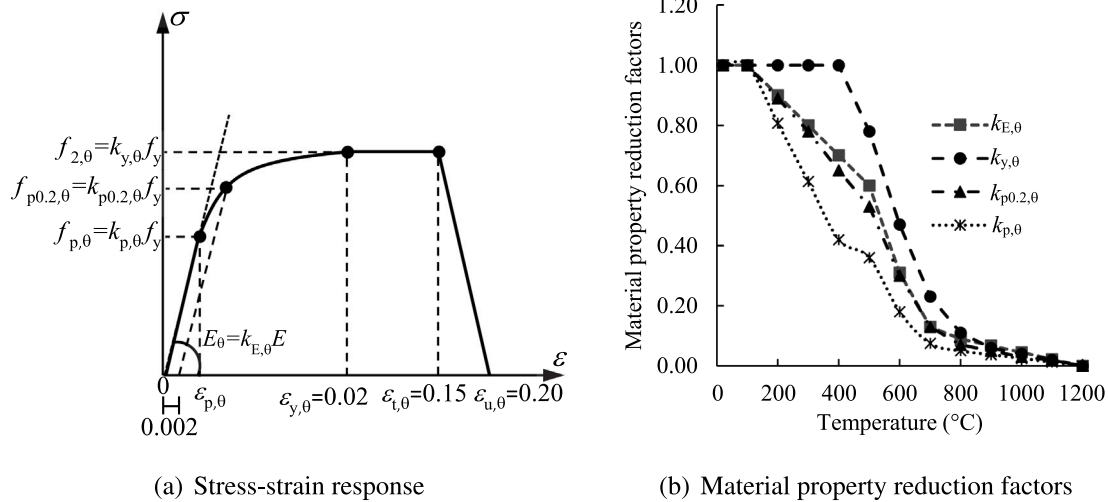


Fig. 1. Stress-strain relationship and material property reduction factors for carbon steel at elevated temperatures adopted in this study as given in [6].

where $k_{E,\theta}$ and $k_{p0.2,\theta}$ are the Young's modulus and 0.2% proof strength reduction factors for carbon steel as given by EN 1993-1-2 [6], $\sigma_{cr,cs}$ is the full cross-section elastic local buckling stress and $\bar{\lambda}_p$ is the room temperature cross-section slenderness. The full cross-section local buckling stress $\sigma_{cr,cs}$ of a steel cross-section can be determined either (i) analytically using the practical formulae put forward in Gardner et al. [20] as described in [13,14] or (ii) numerically using computer software such as the CUFISM [21]; in this paper, the former method is recommended and adopted in the implementation of the proposed method.

2.4. Base curve

To take into account the detrimental influence of local buckling on resistance, the proposed fire design approach requires the design value of the maximum compressive normal strain $\epsilon_{Ed,\theta}$ at each cross-section of a steel member to be smaller than or equal to the CSM compressive strain limit $\epsilon_{csm,\theta}$ at elevated temperature θ as given by

$$\frac{\epsilon_{Ed,\theta}}{\epsilon_{csm,\theta}} \leq 1.0. \quad (4)$$

For the determination of the compressive strain limit $\epsilon_{csm,\theta}$ of a steel member at elevated temperature θ , the proposed fire design method uses a modified continuous strength method (CSM) [22] base curve formulation derived in Murtaza and Kucukler [13] and defined by Eqs. (5) and (6):

$$\frac{\epsilon_{csm,\theta}}{\epsilon_{y,\theta}} = \frac{0.25}{-3.6} + \frac{0.002}{\epsilon_{y,\theta}} \leq \left(\Omega, \frac{C_1}{\epsilon_{y,\theta}} \right) \quad \text{for } \bar{\lambda}_{p,\theta} \leq 0.68, \quad (5)$$

$$\frac{\epsilon_{csm,\theta}}{\epsilon_{y,\theta}} = \left(1 - \frac{0.222}{\bar{\lambda}_{p,\theta}^{-1.05}} \right) \frac{1}{\bar{\lambda}_{p,\theta}^{-1.05}} + \frac{0.002(\sigma/f_{p0.2,\theta})^{n_\theta}}{\epsilon_{y,\theta}} \quad \text{for } 0.68 < \bar{\lambda}_{p,\theta} \leq 1.0, \quad (6)$$

where $\epsilon_{y,\theta}$ is the elevated temperature yield strain calculated by dividing the elevated temperature 0.2% proof strength $f_{p0.2,\theta}$ by the elevated temperature Young's modulus E_θ (i.e. $\epsilon_{y,\theta} = f_{p0.2,\theta}/E_\theta$), σ is the maximum compressive stress and n_θ is the strain hardening parameter. In Eq. (5), the upper limit Ω is equal to 15 and C_1 is set to 0.02 which limits $\epsilon_{csm,\theta}$ to 2% in accordance with the upper strain limit of 2% used for the determination of the reference elevated temperature material strengths in the fire design of steel members in EN 1993-1-2 [6]. It should however be noted that future research will focus on

the necessity of the use of the C_1 factor and 2% upper compressive strain limit in the implementation of the proposed design approach for structural steel systems in fire where the redistribution of internal forces can be of significance. The modified base curve as well as the n_θ values used in Eq. (6) are illustrated in Fig. 2. Note that the adopted base curve formulations are modifications of the CSM base curve used in previous research [14–19] for structural steel design by second-order inelastic analysis at room temperature.

To illustrate the viability of the use of the CSM base curve with modifications to account for the elevated temperature material properties of steel in the proposed fire design method, the relation between the elevated temperature cross-section deformation capacity $\epsilon_{csm,\theta}/\epsilon_{y,\theta}$ and elevated temperature cross-section slenderness $\bar{\lambda}_{p,\theta}$ is investigated herein by employing the results from 115 isothermal fire tests on steel cross-sections reported in the literature. Table 1 shows the experimental studies considered in the derivation of the base curve data for non-slender ($\bar{\lambda}_{p,\theta} \leq 0.68$) and slender ($\bar{\lambda}_{p,\theta} > 0.68$) cross-sections in fire where N is the number of tests carried out in an experimental study. In line with the procedure adopted in the development of the CSM base curve [23], the deformation capacity of a non-slender cross-section ($\bar{\lambda}_{p,\theta} \leq 0.68$) in fire $\epsilon_{csm,\theta}/\epsilon_{y,\theta}$ is determined from the fire tests using Eq. (7):

$$\frac{\epsilon_{csm,\theta}}{\epsilon_{y,\theta}} = \frac{\epsilon_{lb}}{\epsilon_{y,\theta}} = \frac{\delta_u/L - 0.002}{\epsilon_{y,\theta}} \quad \text{for } \bar{\lambda}_{p,\theta} \leq 0.68 \quad (7)$$

where ϵ_{lb} is the elevated temperature local buckling strain equal to the axial shortening of the stub column δ_u at the ultimate load $N_{u,\theta}$ divided by the length of the column L (i.e. $\epsilon_{lb} = \delta_u/L$). Note that 0.2% is subtracted from the local buckling strain ϵ_{lb} (i.e. $\delta_u/L - 0.002$) as shown in Eq. (7) for compatibility with the bi-linear CSM material model for which the original CSM base curve was derived [22]; of course, the EN 1993-1-2 [6] elevated temperature material model is adopted in the proposed fire design method in lieu of the bi-linear CSM material model and the addition of 0.2% to the local buckling strain is made to the base curve formulations as shown in Eqs. (5) and (6) to reverse the subtraction of 0.2%. To determine the elevated temperature deformation capacity $\epsilon_{csm,\theta}/\epsilon_{y,\theta}$ of slender cross-sections ($\bar{\lambda}_{p,\theta} > 0.68$), the concept of the equivalent local buckling strain $\epsilon_{lb,e}$ [24,25] is used as shown in Eq. (8):

$$\frac{\epsilon_{csm,\theta}}{\epsilon_{y,\theta}} = \frac{\epsilon_{lb,e}}{\epsilon_{y,\theta}} = \frac{N_{u,\theta}}{N_{y,\theta}} \quad \text{for } \bar{\lambda}_{p,\theta} > 0.68 \quad (8)$$

in which $N_{y,\theta}$ is the elevated temperature cross-section yield load equal to the elevated temperature 0.2% proof strength $f_{p0.2,\theta}$ multiplied by the cross-section area A (i.e. $N_{y,\theta} = f_{p0.2,\theta}A$). Fig. 3 shows a comparison

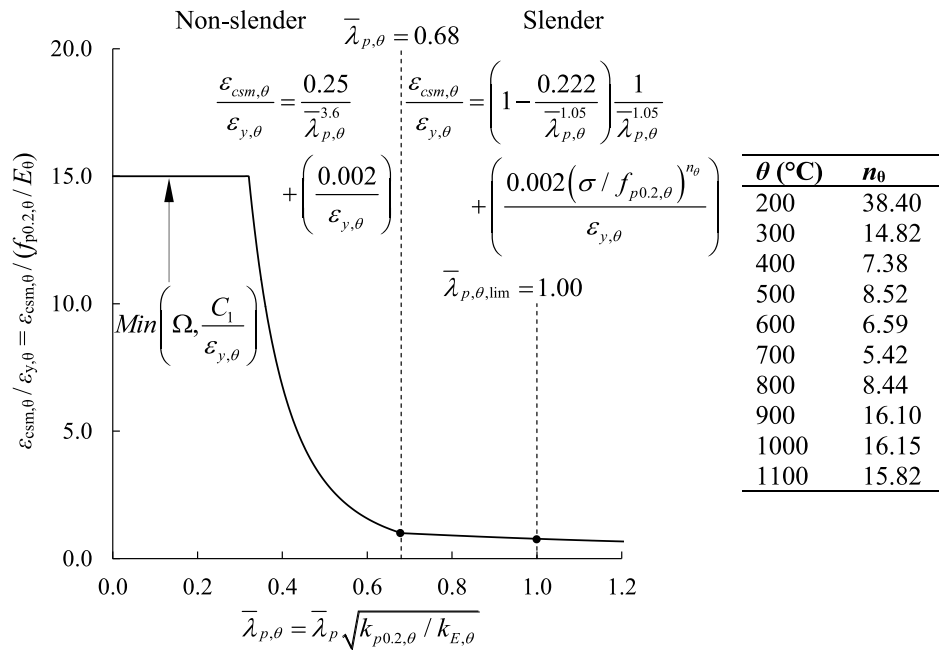


Fig. 2. Base curve modified for elevated temperature design relating the cross-section deformation capacity $\epsilon_{csm,\theta}/\epsilon_{y,\theta}$ to the elevated temperature cross-section slenderness $\bar{\lambda}_{p,\theta}$.

Table 1

Fire tests on stub columns considered for the assessment of the room temperature CSM base curve adopted in the proposed fire design method.

Study	Cross-section & Material	Temperature (°C)	N
Yang et al. [26]	Carbon steel hot-rolled I-section	300, 400, 450, 500, 550, 600	6
Yang and Hsu [27]	Carbon steel welded I-section	500, 550, 600	9
Yang et al. [28]	Fire resistant steel welded SHS & I-section	400, 500, 600	17
Pauli et al. [29]	Carbon steel hot-rolled SHS, RHS & I-section	400, 550, 700	23
Feng et al. [30]	Carbon steel cold-formed channel	250, 400, 550, 700	9
Yang et al. [31]	Fire resistant steel welded I-section	400, 500, 600	9
Wang et al. [32]	Carbon steel welded I-section	450, 650	8
Yang and Yang [33]	Carbon steel welded RHS	500	6
Lan et al. [34]	Stainless steel hot-rolled channel section	300, 450, 600, 750, 850, 1000	12
Su et al. [35]	High strength steel welded I-section	300, 600, 700, 800, 900, 1000	12
Sharhan et al. [36]	High strength steel welded I-section	450, 600	4

of the cross-section deformation capacities obtained from the fire tests described in Table 1 against the CSM base curve for plated cross-sections. As can be seen from the figure, the CSM base curve provides a good fit to the cross-section deformation capacities from the fire tests, verifying the appropriateness of the use of the CSM base curve with modifications to account for the adopted EN 1993-1-2 [6] elevated temperature material model in the proposed fire design method.

2.5. Equivalent geometric imperfections

In the implementation of the proposed fire design method, the modelling of equivalent bow imperfections in steel members is required whereby the detrimental effects of both geometric imperfections and residual stresses are taken into consideration. As developed in [13] based on the equation proposed in [37], the equivalent geometric imperfection for a steel member is calculated as

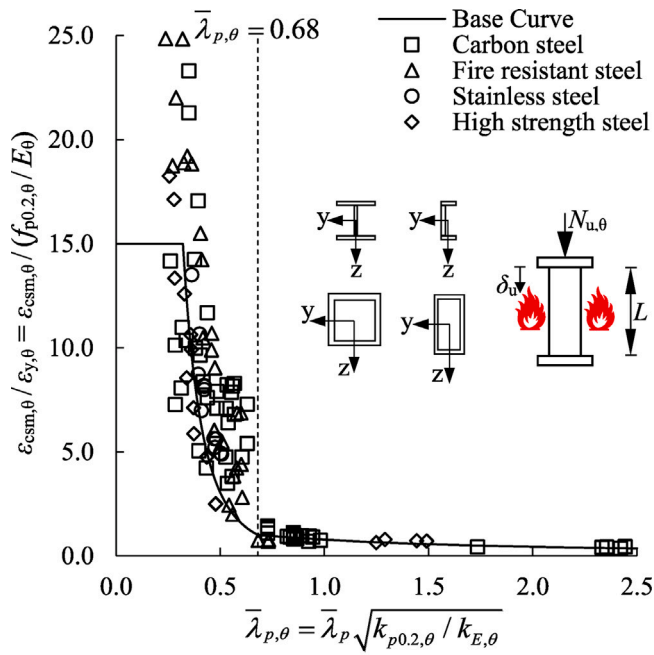
$$e_0 = \alpha\beta L \geq L/1000 \quad \text{with} \quad \beta = \frac{1}{250}, \quad (9)$$

in which α is the imperfection factor equal to $\alpha = 0.65\sqrt{235/f_y}$ as recommended in EN 1993-1-2 [6], $\beta = 1/250$ is the reference bow imperfection and L is the member length. As can be seen in Eq. (9), a lower bound defined for the equivalent imperfection e_0 is taken as $1/1000$ of the member length L (i.e. $e_0 \geq L/1000$), which is equal to the maximum member out-of-straightness permitted in the European standard for the execution of steel structures EN 1090-2 [38]. Note

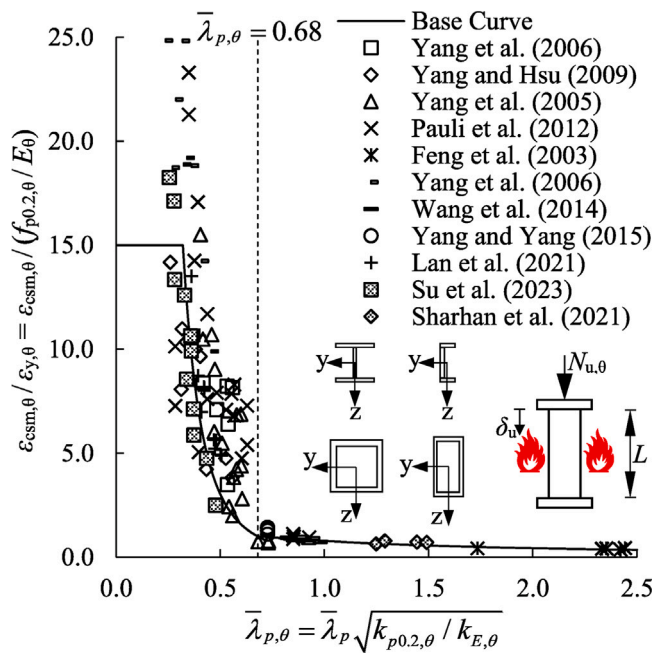
that for beams subjected to pure bending and not susceptible to lateral instability effects, the modelling of the equivalent imperfections is not necessary.

2.6. Strain averaging approach

The cross-section bending moment resistance of a steel member increases when it is under a moment gradient compared to when it is subjected to uniform bending since additional restraint is afforded to the most heavily stressed critical cross-section by the adjacent regions that are under lower stresses. To take this beneficial effect into account, the utilisation of a strain averaging approach is recommended in this paper, whereby the maximum normal strains within the cross-sections of steel members $\epsilon_{Ed,\theta}$ under moment gradients are averaged over the local buckling half-wavelengths of the cross-sections $L_{b,cs}$ and checked against the corresponding strain limits of steel members in fire in accordance with the recommendations of [14]. The local buckling half-wavelength $L_{b,cs}$ of a steel member is determined using the practical formulae put forward in [39]. The strain averaging approach is shown schematically in Fig. 4, employing a cantilever in which the maximum normal strains are averaged over two beam finite elements. Note that in Fig. 4, the maximum strains are averaged by taking into consideration elements 1 and 2 only; the maximum normal strain $\epsilon_{Ed,\theta,3}$ in element 3 is not accounted for in the strain averaging approach as this element is not fully within the local buckling half-wavelength $L_{b,cs}$.



(a) For different materials



(b) For different studies

Fig. 3. Comparison of the base curve against the cross-section deformation capacities from isothermal fire tests on steel stub columns.

The use of the strain averaging approach described in this subsection leads to increased ultimate resistances for steel members subjected to nonuniform bending in fire; conservatively, the design can also be carried out by considering the maximum compressive strains in steel members under nonuniform bending without strain averaging. It is also worth indicating that the maximum permissible lengths of beam finite elements used to model steel members in the implementation of the proposed method should be less than the local buckling half-wavelengths $L_{b,cs}$, thereby both considering the response of structural

steel members in fire accurately and enabling the application of the strain averaging approach if the user opts to utilise it.

2.7. Influence of shear forces on moment resistance

Shear effects greater than half of the elevated temperature shear resistances of steel cross-sections have detrimental influence on their ultimate load carrying capacities in fire according to EN 1993-1-2 [6]. To take the detrimental influence of high shear forces into account in the proposed fire design method, reduced strain limits $\epsilon_{csm,\theta,V}$ are used for cross-sections of steel members subjected to shear forces V_{Ed} greater than half of their elevated temperature cross-section shear resistances $V_{fi,t,Rd}$ (i.e. $V_{Ed} > 0.5V_{fi,t,Rd}$). Similar to the approach adopted in [14], the reduced strain limits $\epsilon_{csm,\theta,V}$ can be determined through the following expression

$$\epsilon_{csm,\theta,V} = \rho_{csm,\theta} \epsilon_{csm,\theta}, \quad (10)$$

where $\rho_{csm,\theta}$ is calculated using Eq. (11):

$$\rho_{csm,\theta} = \begin{cases} 1 & \text{for } V_{Ed} \leq 0.5V_{fi,t,Rd} \\ \frac{0.5}{0.5 + \rho_{\theta}} & \text{for } V_{Ed} > 0.5V_{fi,t,Rd} \end{cases} \quad (11)$$

in which ρ_{θ} and $V_{fi,t,Rd}$ are determined as

$$\rho_{\theta} = \left(\frac{2V_{Ed}}{V_{fi,t,Rd}} - 1 \right)^2, \quad (12)$$

$$V_{fi,t,Rd} = A_v k_{y,\theta} f_y / \sqrt{3}, \quad (13)$$

where A_v is the cross-section shear area that can be obtained using the expressions provided in EN 1993-1-1 [40] and $k_{y,\theta}$ is the elevated temperature reduction factor for the material strength at 2% total strain. Note that the expressions recommended in Quan et al. [17] for the reduction of strain limits due to high shear effects will also be taken into consideration in future research for the application of the proposed design method to steel members subjected to torsion at elevated temperatures.

Fig. 5 shows the comparison of (i) the ultimate bending moment resistances M_u normalised by the cross-section plastic bending moment capacities $M_{pl,\theta}$ (i.e. $M_u/M_{pl,\theta}$) against (ii) the ultimate shear resistances V_u normalised by the cross-section plastic shear resistances $V_{pl,\theta}$ (i.e. $V_u/V_{pl,\theta}$) at 500 °C, determined using shell finite element models, the proposed fire design approach and EN 1993-1-2 [6] for steel beams with IPE 160, IPE 200 and IPE 240 cross-sections and shear length L_s to local buckling half-wavelength $L_{b,cs}$ ratios ranging between 0.5 and 20 (i.e. $0.5 \leq L_s/L_{b,cs} \leq 20$). The elevated temperature moment–shear (M–V) interaction data shown in Fig. 5 illustrate significant reductions in bending moment resistances when the cross-sections are subjected to high shear forces. Comparing the results obtained from the shell finite element models against those determined by the proposed approach in Fig. 5, it can be seen that the proposed method provides safe-sided capacity predictions for steel members under high shear forces at elevated temperatures, which are more accurate than those predicted by EN 1993-1-2 [6] for a high number of cases. Note that in Fig. 5, the differences in the ultimate resistance predictions of the shell and beam finite element models for the bending-dominant cases can be attributed to the beneficial effects of local moment gradients explicitly captured in the shell finite element models as well as the effective increases in material strength under multi-axial stress conditions which were also observed in [14].

2.8. Design procedure

The procedure for the fire design of steel beams and beam–columns through the proposed GMNIA with strain limits based fire design approach is shown in Fig. 6. Design may be carried out using the isothermal analysis technique where the member or structural system is heated and then loaded until failure or the anisothermal analysis

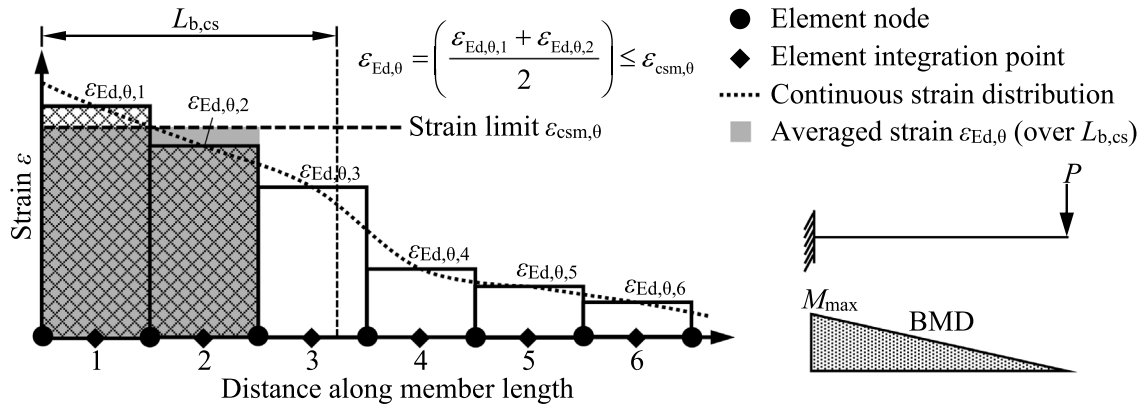


Fig. 4. Strain averaging approach depicted for a cantilever beam modelled using 6 beam finite elements. The averaged maximum normal strain $\epsilon_{Ed,\theta}$ is calculated considering the elements that are completely within the local buckling half-wavelength $L_{b,cs}$; thus, $\epsilon_{Ed,\theta}$ is equal to the average of the maximum normal strain $\epsilon_{Ed,\theta,1}$ in element 1 and the maximum normal strain $\epsilon_{Ed,\theta,2}$ in element 2 (i.e. $\epsilon_{Ed,\theta} = (\epsilon_{Ed,\theta,1} + \epsilon_{Ed,\theta,2})/2$).

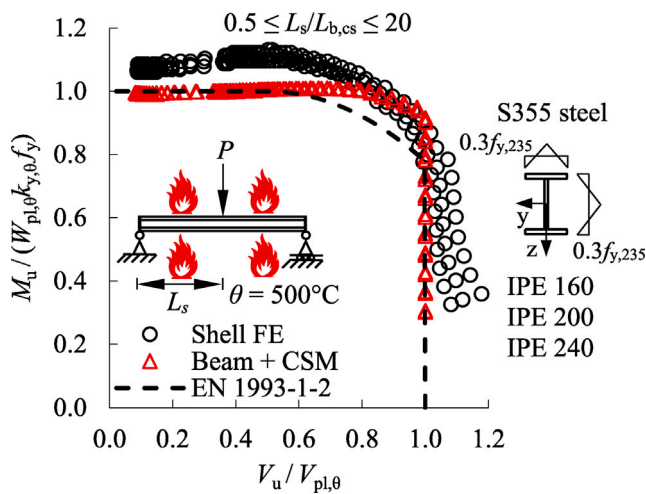


Fig. 5. Moment-shear interaction for IPE beams at 500 °C.

technique where the member or structural system is first loaded and then heated until failure. Note that in the application of the proposed fire design method in this study, the GMNIA of steel beams and beam-columns in fire were carried out through the finite element analysis software Abaqus [41], using the two-noded shear deformable prismatic Timoshenko beam elements. However, any other finite element software package able to carry out the GMNIA of steel members in fire with the capability of considering the spread of plasticity, second-order effects, erosions in strength and stiffness as well as the development of thermal strains at elevated temperatures could be utilised in the implementation of the proposed structural steel fire design approach; this type of software is available in practice such as [42,43].

When the isothermal analysis approach is used in the application of the proposed design method, the elevated temperature strain limits $\epsilon_{csm,\theta}$ should be determined for the predefined elevated temperature value θ and the strain limit checks should be performed at each load increment by checking if the maximum or averaged compressive strains within the cross-sections $\epsilon_{Ed,\theta}$ attain the calculated CSM strain limits $\epsilon_{csm,\theta}$. On the other hand, in the application of the proposed fire design approach through the anisothermal technique, (i) the CSM strain limits $\epsilon_{csm,\theta}$ for steel members should be calculated at each temperature increment by taking into account the temperatures of the cross-sections and (ii) the strain limit checks should be carried out at each temperature increment by checking whether the maximum or averaged strains within the cross-sections $\epsilon_{Ed,\theta}$ attain the calculated CSM strain limits

$\epsilon_{csm,\theta}$. Moreover, the temperatures of steel elements could be increased adopting temperature increase profiles determined either through a separate heat transfer analysis for a particular fire situation or using empirical equations for the temperature increase of steel members such as those provided in EN 1993-1-2 [6] whose accuracy is extensively validated for the cases where the ambient temperatures increase in accordance with the ISO 834-1 [44] temperature-time curve. Where high shear forces are of a concern when using the isothermal and anisothermal analysis approaches, it is necessary to determine the reduction factor for shear $\rho_{csm,\theta}$ and then check if the strains $\epsilon_{Ed,\theta}$ reach the reduced CSM strain limits $\rho_{csm,\theta}\epsilon_{csm,\theta}$. In some cases, the structural fire resistance of restrained steel beams analysed using the anisothermal approach may be governed by deflection criteria instead of strength criteria as large deflections typically occur prior to the strength limit state being achieved which can lead to a loss of fire compartmentation and general structural functionality [45]; such deflection limit states are given in International [44] and British [46] standards. A deflection limit based on [44,46] was adopted in both shell finite element simulations and application of the proposed method in this paper as appropriate.

As shown in Fig. 6, both the isothermal and anisothermal analysis techniques can be adopted in the implementation of the proposed method. It should be emphasised that the use of the anisothermal analysis technique in the implementation of the proposed method provides a more realistic representation of the behaviour of steel members and structures in fire since steel members and structures are first loaded at room temperature and then subjected to heating in a fire situation; the anisothermal analysis approach furnishes the failure (i.e. critical) temperatures and corresponding failure durations for steel members and structures in fire, explicitly demonstrating the performance of a steel member or structure in a particular fire situation. On the other hand, the isothermal analysis technique directly provides ultimate resistances of structural steel members at particular elevated temperature levels. Thus, it can be deemed as practical in situations where the resistances of steel elements within a range of temperature values are necessary; the isothermal analysis technique also readily enables the verification of a fire design approach as proposed in this paper for a range of elevated temperature levels that can be observed in practical situations.

In the application of the proposed GMNIA with strain limits based fire design method, the total strains ϵ_t that develop in structural steel members comprise (i) the mechanical strains ϵ_m and (ii) the thermal strains ϵ_{th} as provided below

$$\epsilon_t = \epsilon_m + \epsilon_{th} \tag{14}$$

It should be emphasised that in the implementation of the proposed fire design method, the compressive mechanical strains ϵ_m should be

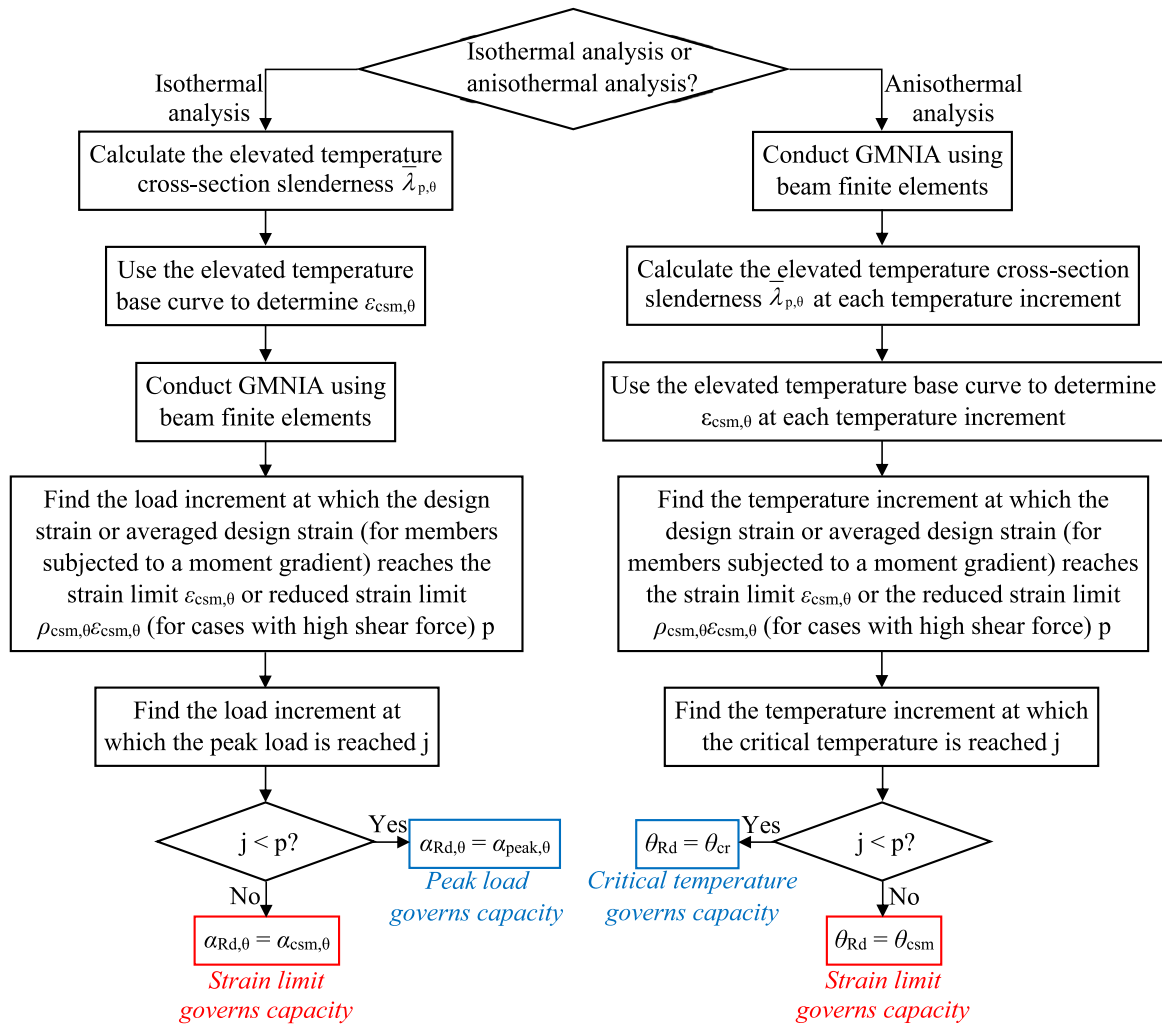


Fig. 6. Procedure for the fire design of steel beams and beam-columns through GMNIA with strain limits at elevated temperatures.

monitored during the analysis in all cases (i.e. $\epsilon_{Ed,\theta} = \epsilon_m$) and compared against the elevated temperature strain limits $\epsilon_{csm,\theta}$. Finite element analysis software packages such as Abaqus [41] provide the mechanical and thermal strains induced in structural steel members separately, thus readily enabling the implementation of the proposed fire design approach.

3. Finite element modelling

In this section, shell finite element models capable of simulating the structural response of steel beams and beam-columns at elevated temperatures are developed and validated against experimental results. In the following sections, the shell finite element models are utilised for the verification of the proposed fire design approach by GMNIA with strain limits.

3.1. Development of shell finite element models

The finite element analysis software Abaqus [41] was used to create shell finite element models capable of replicating the structural response of steel beams and beam-columns at elevated temperatures. To accurately capture the behaviour of the steel members in fire, sixteen four-noded reduced integration S4R elements were used to model the flange and web plates of I-sections which was also adopted in previous studies for similar applications [47–49]; the numbers of elements in the longitudinal direction were defined such that an element aspect

ratio of approximately one was achieved in the web plates. The shell finite element models used the EN 1993-1-2 [6] elevated temperature material model for carbon steel in conjunction with the corresponding material reduction factors. As for the geometric imperfections which were directly defined in the shell finite element models, magnitudes of 1/1000 of the member lengths L were used for the member out-of-straightness and the local imperfection magnitudes e_0 were taken as 1/200 (i.e. $e_0 = b/200$) of the plate widths in accordance with [14,18,50] as shown in Fig. 7. The local imperfections were defined in the shell finite element models by (i) first assigning the imperfection magnitude of $b/200$ to the critical plate (i.e. flange or web plate) with the lower elastic buckling stress $\sigma_{cr,p}$ and (ii) then assigning an appropriate imperfection magnitude to the non-critical plate such that the 90° angle at the flange-web junction is maintained. Note that the local buckling half-wavelengths $L_{b,cs}$ were determined in accordance with [39]. It is also worth noting that the local imperfection magnitudes can be regarded as equivalent imperfections [51], therefore some conservatism may be expected in the ultimate resistance predictions determined using the shell finite element models in certain cases. Residual stresses were defined in the models for hot-rolled and welded I-section steel members by adopting the ECCS residual stress patterns [52]. In the finite element simulations, both (i) the isothermal analysis technique which involves the increase of temperature up to a fixed value followed by the incremental application of the load using the modified Riks method [41] and (ii) the anisothermal analysis technique where the load is first applied up to a fixed value followed by heating were

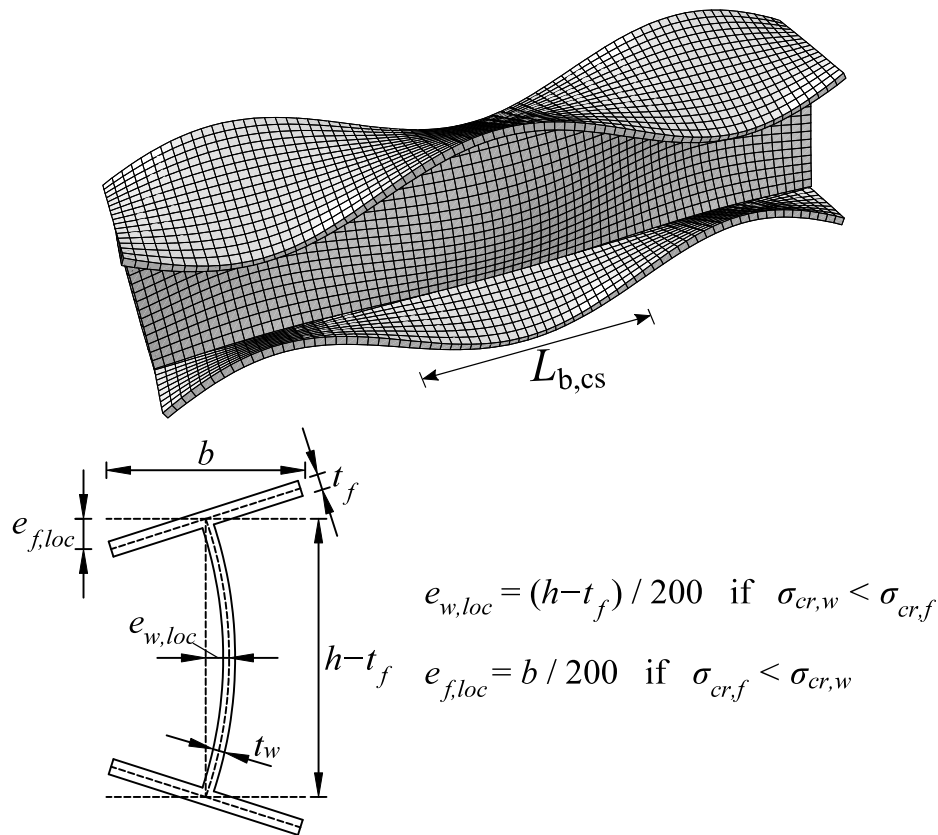


Fig. 7. Local geometric imperfections used within shell finite element models.

utilised. Note that in the case of the anisothermal analyses of the shell finite element models, the temperatures of the steel members were increased using the temperature development profiles obtained from the prior heat transfer analyses where the ambient temperature was increased adopting the ISO 834 [44] temperature–time curve, similar to the approach adopted in other studies [53].

Fig. 8 shows the support conditions adopted for steel beams and beam–columns in this study where Δ are the translations, φ are the rotations, k_{Δ} is the axial spring stiffness of the translational springs, $k_{\varphi,b}$ is the rotational spring stiffness of the rotational springs used for the beams and $k_{\varphi,c}$ is the rotational spring stiffness of the rotational springs used for beam–columns. Lateral–torsional buckling was prevented in the beams and beam–columns subjected to major axis bending by restraining the translations of the nodes at the centre of the flanges in the y direction (i.e. $\Delta_y = 0$). For steel beam–columns, the β factor is used to define the magnitude of the applied axial compression force N_{Ed} and the bending moment M_{Ed} as shown in Fig. 8, which will be explained in detail in the following sections.

3.2. Validation of shell finite element models

Results from fire tests on steel beams from the literature were used to validate the shell finite element models utilised in this paper. The geometric and material properties, support conditions and the imperfection magnitudes of the specimens reported in the considered experimental studies were used within the numerical models. For the cases where the elevated temperature material response of a specimen was not provided, the EN 1993-1-2 [6] material model was used. Moreover, in the cases without the provision of the geometric imperfections, the imperfection magnitudes described in Section 3.1 were used. Note that the finite element modelling approach adopted in this paper has also been validated previously in [54–59].

3.2.1. Validation against isothermal experiments carried out on I-section beams

Dharma and Tan [60] conducted isothermal experiments on hot-rolled or welded I-section steel beams tested at 415 °C or 615 °C. The beams were tested under simply-supported boundary conditions with lateral restraints placed at different locations, thereby assessing the behaviour for different unrestrained lengths L_E . Table 2 compares the ultimate mid-span moments from the fire tests $M_{u, test}$ and those determined through the shell finite element models created herein $M_{u, FE}$. The good agreement between $M_{u, FE}$ and $M_{u, test}$ in Table 2 for the specimens indicates that the developed shell finite element models are capable of predicting the behaviour of steel beams in fire.

3.2.2. Validation against anisothermal experiments carried out on restrained I-section beams

Liu et al. [61] carried out anisothermal experiments on $178 \times 102 \times 19$ UB steel (grade S275) beams. Axial restraints of 8 kN/mm, 35 kN/mm or 62 kN/mm were utilised during testing and beams were connected to the frame assembly through web cleat connections or end-plate connections. Fig. 9 presents the temperature–deflection paths achieved experimentally and those derived from the finite element models created in this study. As can be seen in Fig. 9, there is a good correlation between the experimental and finite element (FE) model curves, indicating that the finite element models developed in this study are capable of replicating the behaviour of steel beams in fire. Note that the differences between the experimental and numerical temperature–displacement paths in Fig. 9 can be ascribed to the early yielding occurring in some of the benchmark shell finite element models; the early yielding observed in the shell finite element models may result from the adoption of the EN 1993-1-2 [6] elevated temperature material model for carbon steel in the numerical simulations since the exact elevated temperature material stress–strain response of the tested specimens was not reported in Liu et al. [61].

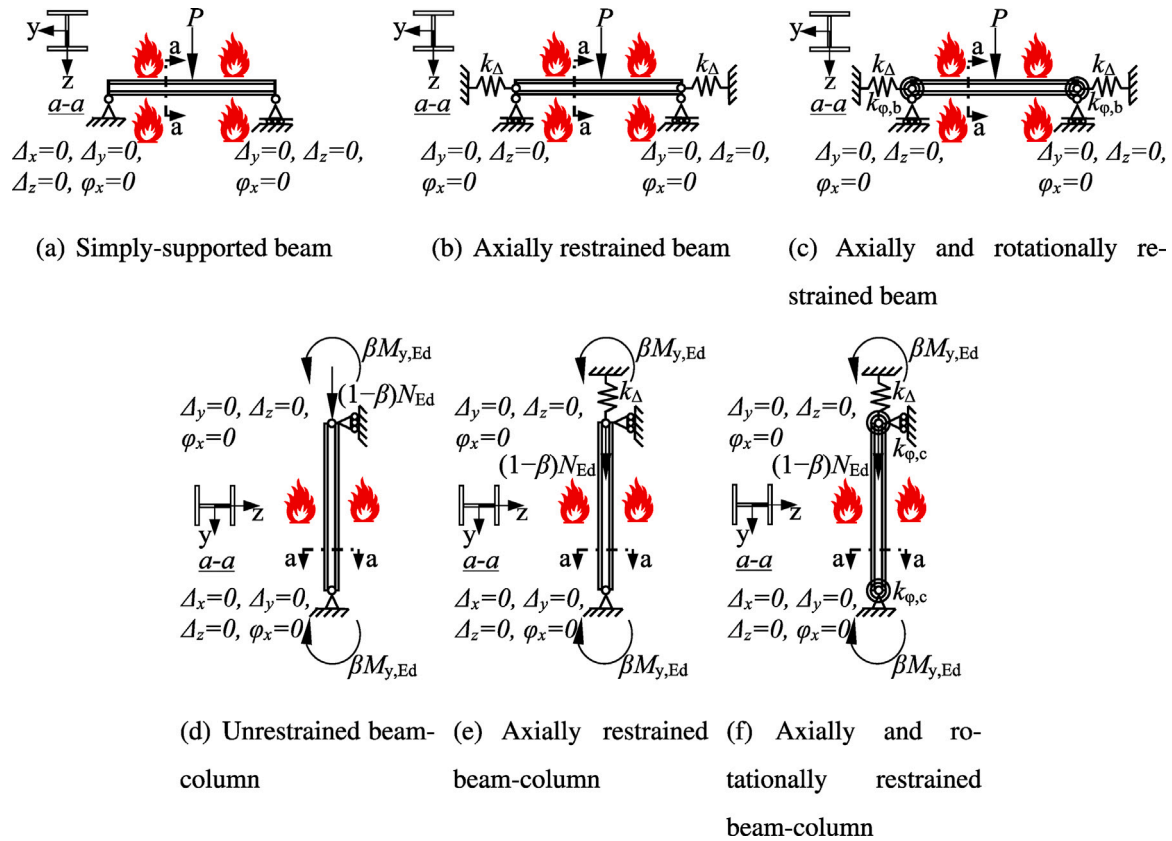


Fig. 8. Support conditions for I-section beams and beam-columns.

Table 2

Comparison of the ultimate moments obtained from the finite element models $M_{u,FE}$ against those obtained from the experiments $M_{u,est}$ by Dharma and Tan [60].

Specimen	Section	Type	L_E (m)	θ (°C)	$M_{u,est}$ (kNm)	$M_{u,FE}$ (kNm)	$M_{u,FE}/M_{u,est}$
S1-1	305 × 165UB54	Hot-rolled	0.650	415	265	260	0.98
S1-2	305 × 165UB54			615	110	110	1.01
S2-1	305 × 165UB54	Hot-rolled	1.725	415	263	263	1.00
S2-2	305 × 165UB54			615	112	116	1.03
S3-2	276 × 163 × 10 × 8	Welded	0.605	415	156	158	1.01
S3-3	276 × 163 × 10 × 8			615	68	69	1.00
S4-1	406 × 178UB54	Hot-rolled	0.650	415	451	435	0.96
S4-2	406 × 178UB54			615	186	187	1.01
Average							1.00
COV							0.019

4. Accuracy assessment of the proposed design method for steel beams in fire

In this section, the accuracy of the proposed GMNIA with strain limits based fire design approach implemented using beam finite element models is assessed using the benchmark structural performance data generated through the validated shell finite element models. Design predictions from the simple calculation models of EN 1993-1-2 [6] are also provided to compare the proposed method against EN 1993-1-2 [6]. Note that henceforth, the ultimate resistance predictions determined through the simple calculation models of EN 1993-1-2 [6] will be referred to as EN 1993-1-2 [6] ultimate resistance predictions considering that in the great majority of cases, the simple calculation models of EN 1993-1-2 [6] are adopted for the fire design of steel structures in practice.

4.1. Isothermal analysis technique

The accuracy of the proposed method is assessed in this subsection for the fire design of steel beams analysed adopting the isothermal analysis technique where the steel beams were first heated up to predefined temperature levels and then loaded until failure. Table 3 shows the parameters considered in the verification of the proposed fire design approach when applied to steel beams using the isothermal analysis method. The parametric study comprised (i) three types of bending cases: 3-point bending, 4-point bending and uniform bending considering both major and minor axis bending, (ii) hot-rolled and welded I-sections, (iii) elevated temperature cross-section slenderness $\bar{\lambda}_{p,\theta}$ values ranging between 0.2 and 1.1 (i.e. $0.2 < \bar{\lambda}_{p,\theta} < 1.1$), (iv) three elevated temperature levels of 300 °C, 500 °C and 700 °C and (v) various shear length L_s to local buckling half-wavelength $L_{b,cs}$ ratios (i.e. $L_s/L_{b,cs}$). Grade S355 steel was used in the parametric studies. Note that the elevated temperature levels of 300 °C, 500 °C

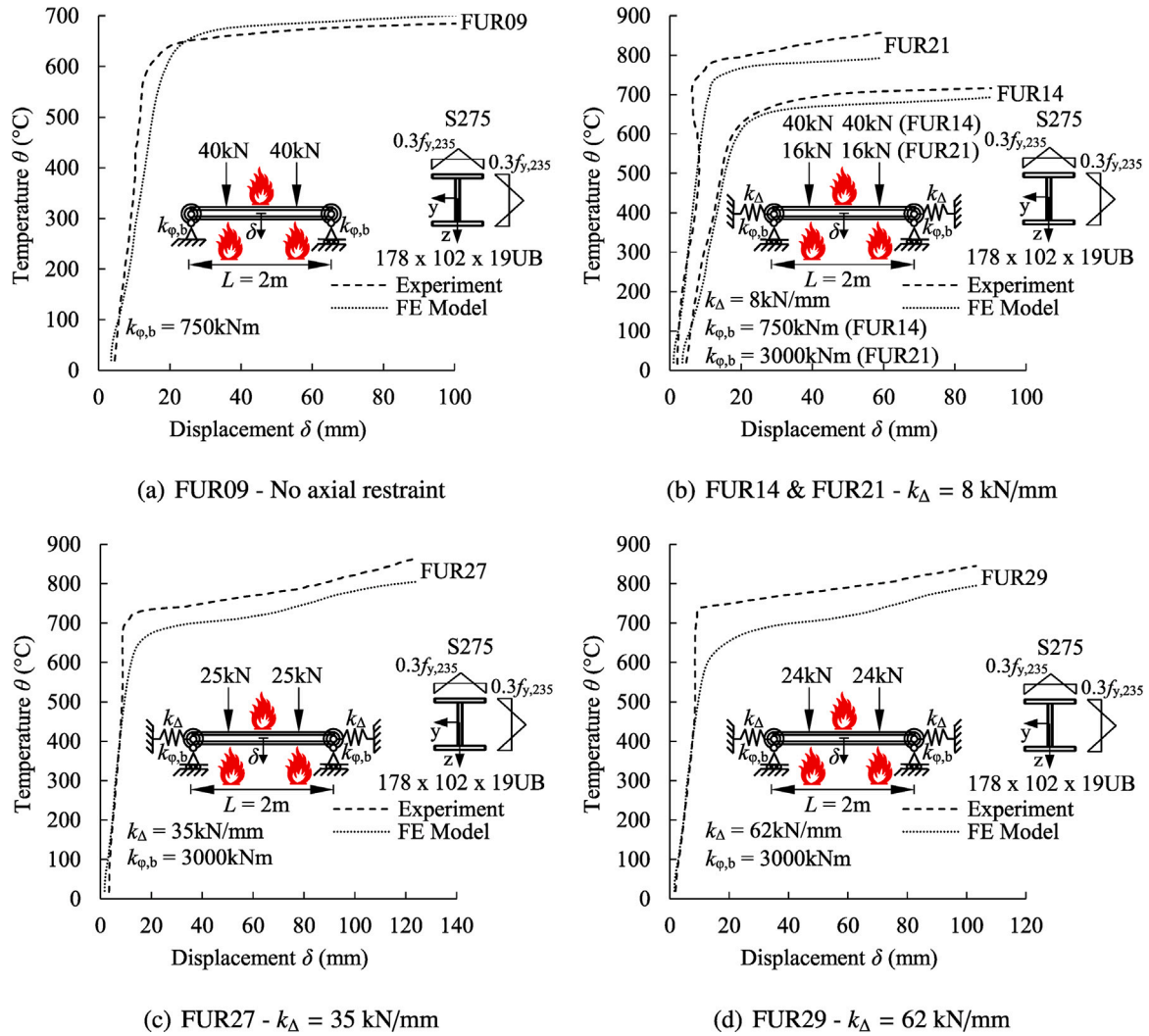


Fig. 9. Comparison between the load versus mid-span displacement paths from Liu et al. [61] anisothermal fire tests and finite element models for restrained I-section steel beams.

and 700 °C were adopted based on typical values used in previous research [8,9,11,12,62–67] considering elevated temperature ranges observed in steel structures in fire.

Figs. 10 and 11 show the accuracy of the proposed fire design method against the benchmark capacity predictions determined through the shell finite element models for hot-rolled I-section beams with a range of elevated temperature cross-section slendernesses $\bar{\lambda}_{p,\theta}$; the capacity predictions from the European structural steel fire design standard EN 1993-1-2 [6] are also included in the figure. In Figs. 10 and 11, the bending moment resistance predictions obtained from the shell finite element models, the proposed method and EN 1993-1-2 [6] $M_{Rd,\theta}$ are normalised by the cross-sectional plastic bending moment resistance $M_{pl,\theta}$ equal to the product of the plastic section modulus W_{pl} , the reduction factor for the yield strength $k_{y,\theta}$ and the yield strength f_y (i.e. $M_{pl,\theta} = W_{pl}k_{y,\theta}f_y$). The flange and web thicknesses of the considered I-sections were defined such that the plate slendernesses of the web plates $\bar{\lambda}_{p,w}$ and flange plates $\bar{\lambda}_{p,f}$ were equivalent (i.e. $\bar{\lambda}_{p,w} = \bar{\lambda}_{p,f}$); this ensured the most critical local buckling scenario with the least interaction between the cross-section elements in the verification of the proposed fire design method. The chosen approach with equivalent plate slendernesses would not be expected to have a very significant effect on the results with respect to the accuracy assessment of the proposed method since the proposed approach accounts for cross-section element interactions in the determination of the elevated temperature cross-section slendernesses $\bar{\lambda}_{p,\theta}$. The design

predictions from the proposed method shown in Fig. 10 accounted for the effects of moment gradients through the use of the strain averaging approach described in Section 2.6. Figs. 10 and 11 demonstrate that the proposed fire design method provides considerably more accurate and consistent ultimate resistance predictions for steel beams at elevated temperatures compared to EN 1993-1-2 [6]. It should be noted that some of the conservative predictions of the proposed method in Figs. 10 and 11 for increasing temperatures and cross-section slendernesses may result from the adopted base curve leading to conservative estimations of strain limits $\epsilon_{csm,\theta}$ for high elevated temperature levels and cross-section slendernesses. Moreover, in the application of the proposed method, the strain limits $\epsilon_{csm,\theta}$ for I-sections subjected to minor axis bending are determined on the basis of the elevated temperature cross-section slendernesses $\bar{\lambda}_{p,\theta}$ with conservative estimations of the influence of the strain gradients in the flanges on ultimate resistances. The presence of strain gradients within the flanges can lead to pronounced plastification of the flanges of slender I-sections under minor axis bending and considerably increase the cross-section minor axis bending moment resistances. The conservative estimations of the influence of strain gradients on the plastification of the flanges lead to somewhat lower ultimate resistance predictions of the proposed method compared to the benchmark shell finite element results for cross-sections with high cross-section slendernesses as seen in Fig. 11. However, it should be emphasised that the proportions of these highly slender cross-sections are typically outside of the ranges used in practice; the elevated

Table 3

Parameters considered in the investigation of the accuracy of the proposed design approach for steel beams analysed adopting the isothermal analysis technique.

Loading conditions & cross-section	Cross-section slenderness $\bar{\lambda}_{p,\theta}$	Temperature θ (°C)	$L_s/L_{b,cs}$
	0.2-1.1	300, 500, 700	10, 12.5, 15, 17.5, 20
	0.2-1.1	300, 500, 700	10
	0.2-1.1	300, 500, 700	20

temperature cross-section slendernesses $\bar{\lambda}_{p,\theta}$ of the most slender cross-sections from the standard range of European sections are less than 0.6 (i.e. $\bar{\lambda}_{p,\theta} < 0.6$) when they are subjected to minor axis bending. It is also worth mentioning that due to the effective enhancement of the elevated temperature material strengths under multi-axial stress conditions as discussed in [14], the bending moment resistance predictions $M_{Rd,\theta}$ of some stocky cross-sections (i.e. $\bar{\lambda}_{p,\theta} < 0.4$) in Fig. 10 are greater than the elevated temperature cross-sectional plastic bending moment resistances $M_{pl,\theta}$ (i.e. $M_{Rd,\theta}/M_{pl,\theta} > 1.0$); similar results have also been observed in previous research [60].

In addition to the results shown in Figs. 10 and 11, Table 4 shows the ratios of the ultimate resistance predictions obtained from the benchmark shell finite element models $M_{Rd,\theta,shell}$ to those determined using the proposed method $M_{Rd,\theta,prop}$ (i.e. $M_{Rd,\theta,shell}/M_{Rd,\theta,prop}$) for all the considered hot-rolled and welded I-section steel beams analysed using the isothermal analysis approach; the ratios of the benchmark shell finite element model capacity predictions $M_{Rd,\theta,shell}$ to those determined through EN 1993-1-2 [6] $M_{Rd,\theta,EC3}$ (i.e. $M_{Rd,\theta,shell}/M_{Rd,\theta,EC3}$) are also displayed in the table; N refers to the number of considered beams. As can be seen from Table 4, the proposed GMNIA with strain limits based fire design approach leads to significantly more accurate and consistent bending moment resistance predictions relative to EN 1993-1-2 [6].

4.2. Anisothermal analysis technique

In this subsection, the accuracy of the proposed fire design approach is investigated for the fire design of simply-supported, axially restrained and axially and rotationally restrained steel beams tested under 3-point bending and analysed using the anisothermal analysis method whereby steel beams are first loaded and then heated up to failure. Table 5 shows the parameters considered in the verification of the proposed fire design approach when applied to steel beams using the anisothermal analysis technique. As can be seen from Table 5, the parameters considered in the parametric studies consisted of (i) hot-rolled and welded I-sections, (ii) a shear length L_s to local buckling half-wavelength $L_{b,cs}$ ratio equal to 10 (i.e. $L_s/L_{b,cs} = 10$), (iii) load intensity α_M of 0.50 (i.e. $\alpha_M = M_{Ed}/M_{c,Rd} = (PL/4)/M_{c,Rd} = 0.50$ where M_{Ed} is the maximum applied bending moment and $M_{c,Rd}$ is the room temperature cross-section bending moment resistance calculated in accordance with EN 1993-1-1 [40]), (iv) cross-section slendernesses $\bar{\lambda}_p$ ranging between 0.2 and 1.1 (i.e. $0.2 < \bar{\lambda}_p < 1.1$), (v) axially and rotationally unrestrained (simply-supported) beams, (vi) axially restrained beams with axial restraint ratios α_Δ of 0.02, 0.10 and 0.30 (i.e. $\alpha_\Delta = k_\Delta/(EA/L) = 0.02, 0.10$ and 0.30), (vii) axially and rotationally restrained beams with rotational restraint ratios $\alpha_{\varphi,b}$ equal to 0.20 and 0.50 (i.e. $\alpha_{\varphi,b} = k_{\varphi,b}/(EI/L) = 0.20$ and 0.50) and axial restraint ratios α_Δ of 0.02, 0.05, 0.10 and 0.30 (i.e. $\alpha_\Delta = k_\Delta/(EA/L) = 0.02, 0.05, 0.10$ and 0.30). The considered parameters are similar to those used

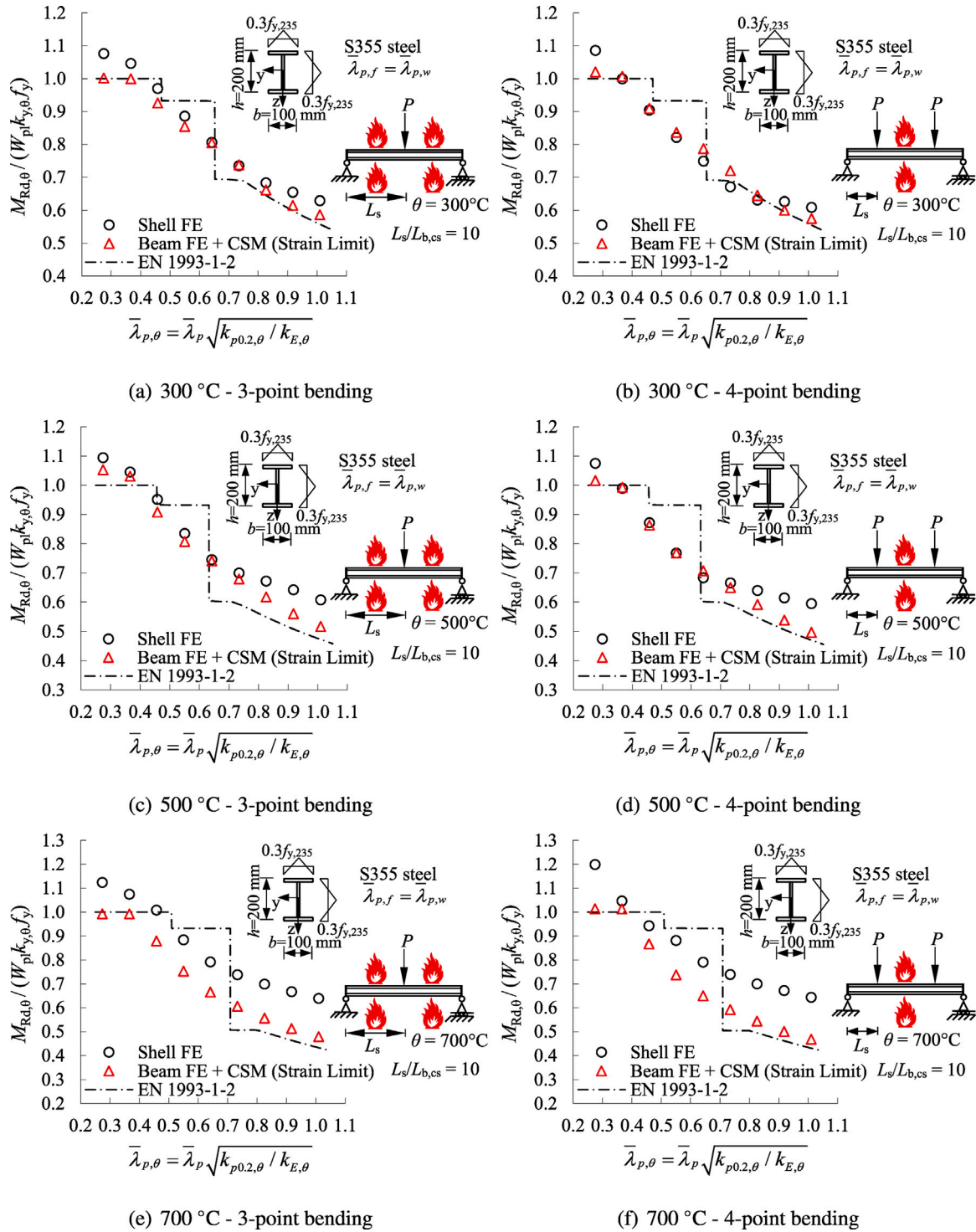


Fig. 10. Capacity predictions achieved using the proposed method and shell finite element models for hot-rolled steel beams tested under 3-point and 4-point bending setups and analysed adopting the isothermal analysis method.

in previous studies [68,69] and A , I and L used to determine the axial restraint α_d and rotational restraint $\alpha_{\phi,b}$ ratios shown in Table 5 are the cross-section area, second-moment of area and length of a steel beam, respectively.

Fig. 12 illustrates the limit temperatures θ_{Rd} obtained from the shell finite element models and those determined through the proposed fire design approach which are plotted against the cross-section slenderness $\bar{\lambda}_p$ for simply-supported, axially restrained and axially and rotationally restrained beams. In addition to the load intensity

α_M values shown in Table 5, a range of additional load intensities α_M are also used in Fig. 12. As can be seen from the figure, the proposed fire design approach generally provides quite accurate and safe-sided limit temperature θ_{Rd} predictions for simply-supported, axially restrained and axially and rotationally restrained steel beams in fire. In addition to the results illustrated in Fig. 12, Table 6 shows the ratios of the limit temperatures θ_{Rd} from the benchmark shell finite element models $\theta_{Rd,shell}$ to those achieved using the proposed fire design method $\theta_{Rd,prop}$ (i.e. $\theta_{Rd,shell}/\theta_{Rd,prop}$) and EN 1993-1-2 [6]

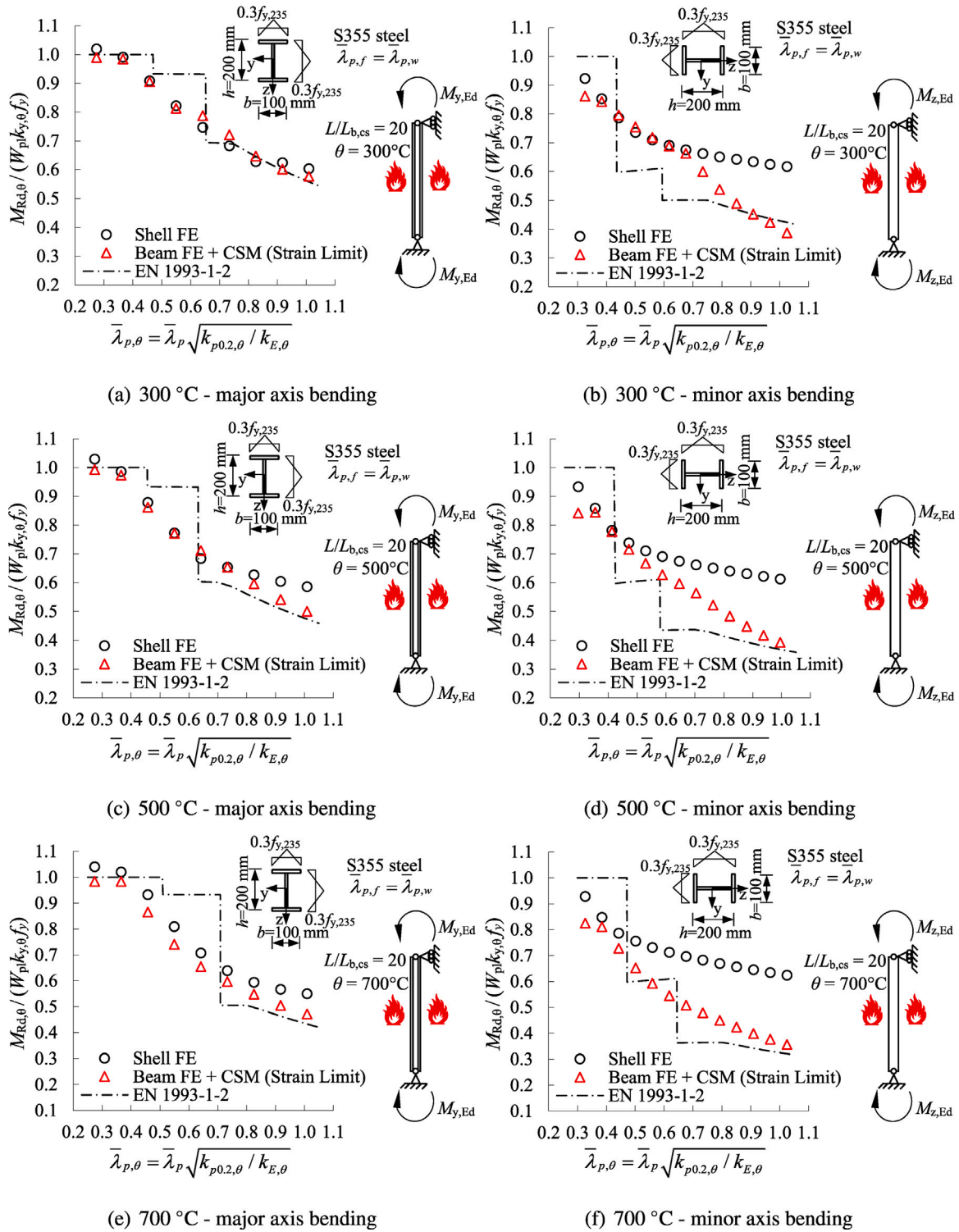


Fig. 11. Capacity predictions achieved using the proposed method and shell finite element models for hot-rolled steel beams subject to a uniform bending moment and analysed adopting the isothermal analysis method.

$\theta_{Rd,EC3}$ (i.e. $\theta_{Rd,shell}/\theta_{Rd,EC3}$) for all the considered unrestrained, axially restrained and axially and rotationally restrained steel beams in the parametric studies (see Table 5); the data in Table 6 is also graphically illustrated in Fig. 13 from which the accuracy of the proposed fire design method and EN 1993-1-2 [6] can be visually compared. As can be seen from Table 6 and Fig. 13, the proposed GMNIA with strain limits fire design approach provides more accurate capacity predictions compared to EN 1993-1-2 [6]. It should be noted that the results from

the proposed method become rather conservative for steel beams with slender cross-sections (i.e. $\bar{\lambda}_p > 0.68$) and high axial restraint ratios. This occurs since the capacity predictions from the proposed fire design method are generally governed by the attainment of strain limits $\epsilon_{csm,\theta}$ which correspond to the temperature at which local buckling first occurs for steel beams with high axial restraints k_Δ and slender cross-sections with $\bar{\lambda}_p > 0.68$; in contrast, in similar cases, the capacities from the benchmark shell finite element models were governed by the

Table 4

Capacity predictions achieved using the proposed method and EN 1993-1-2 [6] compared with benchmark shell finite element model predictions for hot-rolled and welded I-section steel beams at elevated temperatures tested under in-plane bending with isothermal conditions.

Type	θ (°C)	N	$M_{Rd,\theta,shell} / M_{Rd,\theta,EC3}$				$M_{Rd,\theta,shell} / M_{Rd,\theta,prop}$			
			Mean	CoV	Max	Min	Mean	CoV	Max	Min
3-point bending		1020	1.17	0.191	1.97	0.82	1.11	0.131	1.61	0.88
4-point bending	300, 500,	204	1.09	0.168	1.59	0.79	1.04	0.104	1.38	0.87
Uniform bending (major)	700	102	0.87	0.111	1.04	0.71	1.04	0.055	1.18	0.93
Uniform bending (minor)		180	1.35	0.119	1.64	1.00	1.24	0.165	1.75	0.96
Total		1506	1.16	0.198	1.97	0.71	1.11	0.141	1.75	0.87

Table 5

Parameters considered in the investigation of the accuracy of the proposed design approach for steel beams analysed adopting the anisothermal analysis technique.

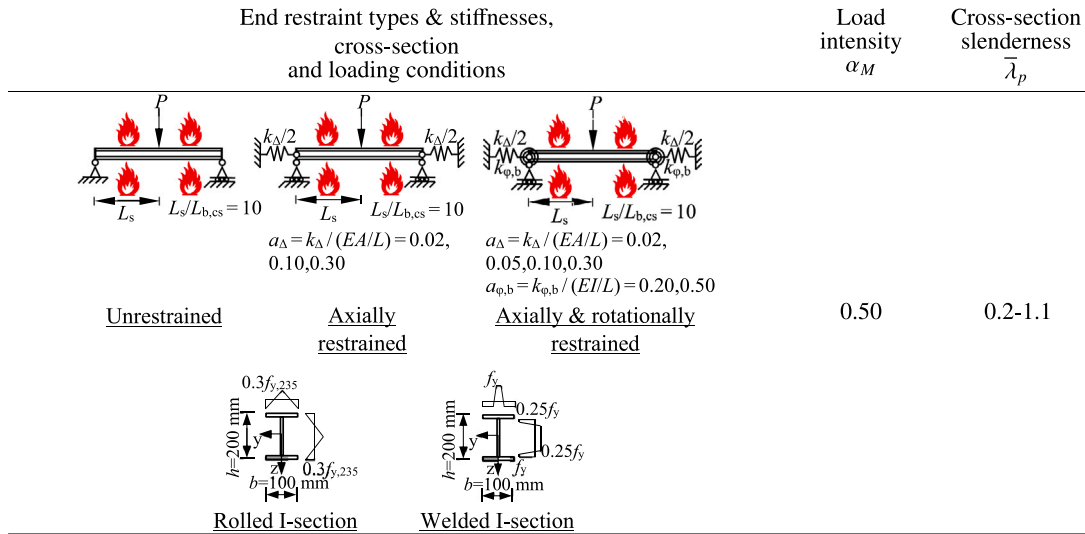


Table 6

Comparison of the critical temperature predictions obtained through the proposed method and EN 1993-1-2 [6] against those determined through the benchmark shell finite element models for hot-rolled and welded steel beams at elevated temperatures analysed adopting the anisothermal analysis approach.

Type	Boundary conditions	N	$\theta_{Rd,shell} / \theta_{Rd,EC3}$				$\theta_{Rd,shell} / \theta_{Rd,prop}$			
			Mean	CoV	Max	Min	Mean	CoV	Max	Min
3-point bending	Unrestrained (Simply-supported)	22	1.01	0.037	1.07	0.94	1.01	0.037	1.16	0.98
	Axially restrained	58	0.89	0.085	1.04	0.74	1.02	0.091	1.33	0.92
	Axially & Rotationally restrained	152	1.07	0.084	1.27	0.86	1.11	0.097	1.51	0.97
Total		232	1.02	0.110	1.27	0.74	1.08	0.101	1.51	0.92

attainment of the adopted deflection limit of ISO 834-1 [44] and BS 476-20 [46], which account for post-buckling behaviour and result in enhanced limit temperatures θ_{Rd} . However, as can be seen from Fig. 13 for steel beams with cross-section slendernesses within the practical range of $0.2 < \bar{\lambda}_p < 0.8$ considering the European standard sections, the proposed GMNIA with strain limits fire design approach leads to accurate limit temperature θ_{Rd} predictions which are both safer and more consistent than those obtained using EN 1993-1-2 [6].

5. Accuracy assessment of the proposed design method for steel beam-columns in fire

In this section, the accuracy of the proposed fire design approach is investigated for the fire design of steel beam-columns analysed adopting the isothermal and anisothermal analysis methods. A high number of steel beam-columns were considered, taking into consideration different cross-section shapes, loading conditions, elevated temperature levels and axially and rotationally unrestrained, axially restrained and axially and rotationally restrained beam-columns.

5.1. Isothermal analysis technique

Table 7 shows the parameters used in the verification of the proposed fire design approach for beam-columns assessed using the isothermal analysis approach. The parametric study considered (i) three loading conditions which were uniform major axis bending plus axial compression, uniform minor axis bending plus axial compression and linearly varying major axis bending plus axial compression with the end moment ratio of 0.5, (ii) hot-rolled and welded IPE 300, HEB 300 and HEAA 300 sections, (iii) three elevated temperature levels of 300 °C, 500 °C and 700 °C, (iv) three elevated temperature member slenderness $\bar{\lambda}_\theta$ values equal to 0.5, 1.0 and 1.5 (i.e. $\bar{\lambda}_\theta = 0.5, 1.0, 1.5$) where $\bar{\lambda}_\theta$ is calculated as

$$\bar{\lambda}_\theta = \bar{\lambda} \sqrt{\frac{k_{y,\theta}}{k_{E,\theta}}} \tag{15}$$

in which $\bar{\lambda}$ is the room temperature slenderness for flexural buckling for the corresponding bending axis and $k_{y,\theta}$ and $k_{E,\theta}$ are the yield strength

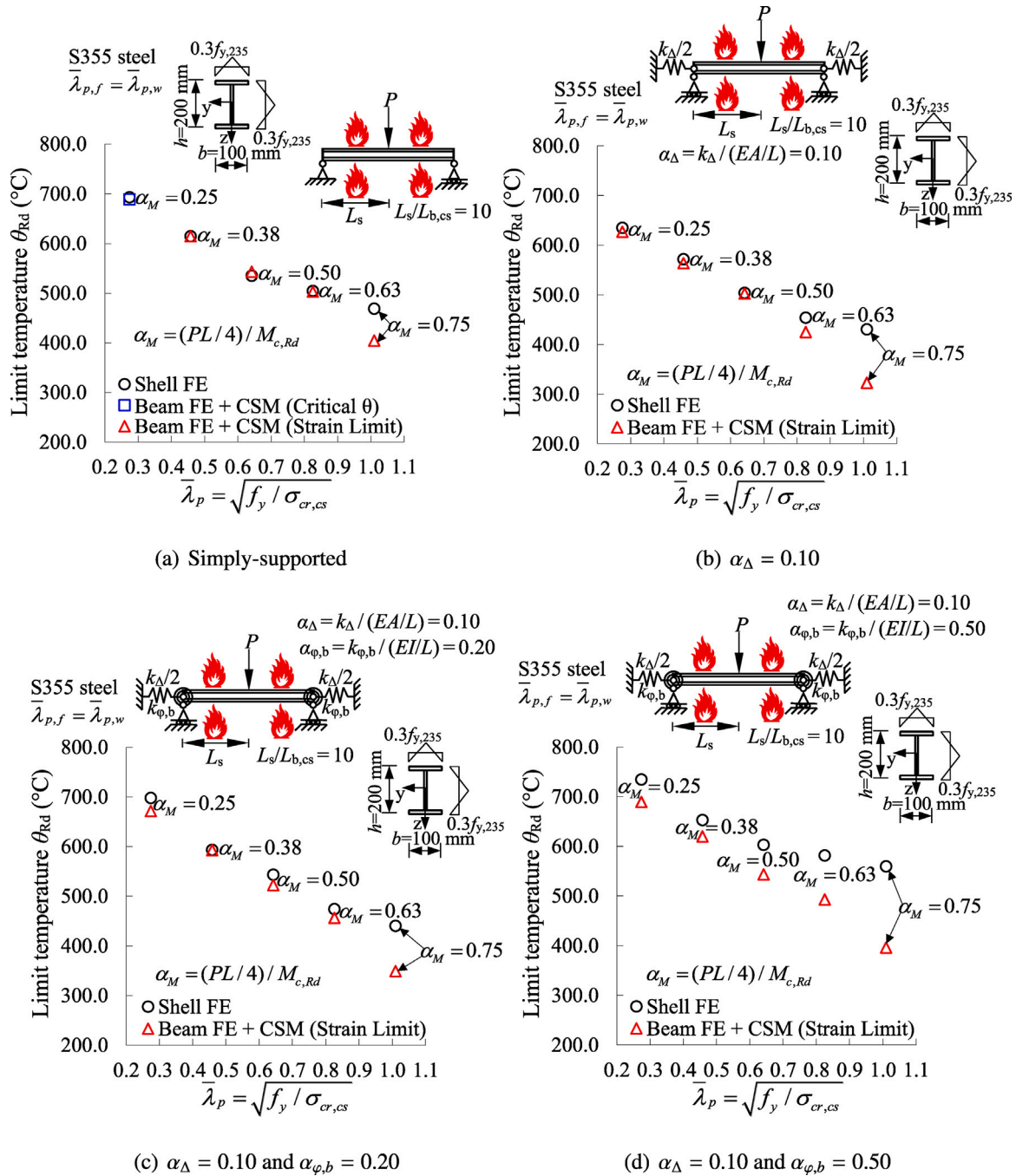
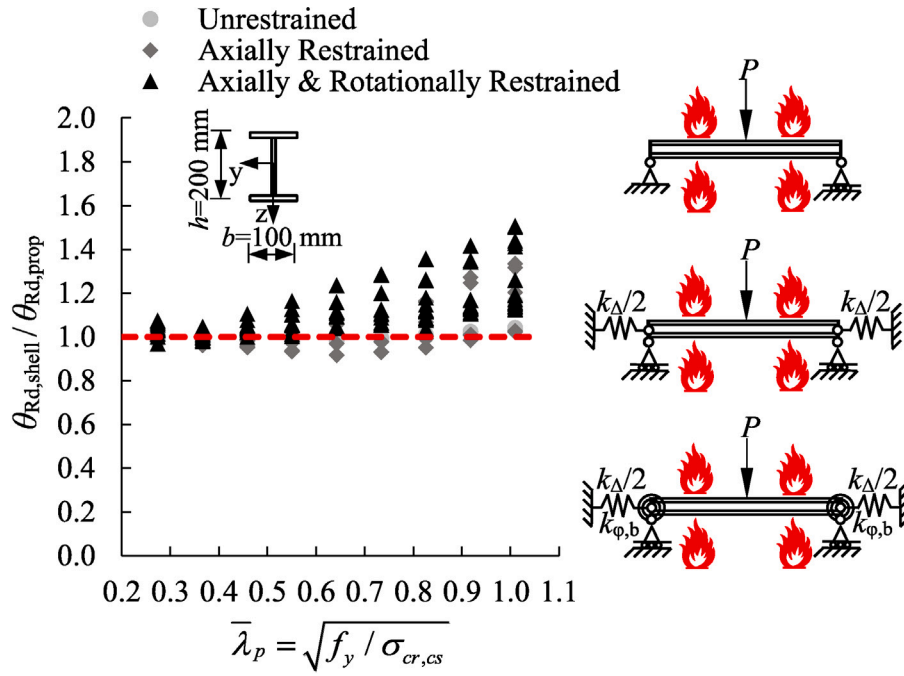


Fig. 12. Capacity predictions of the proposed method and benchmark shell finite element models for hot-rolled I-section steel beams analysed using the anisothermal analysis method.

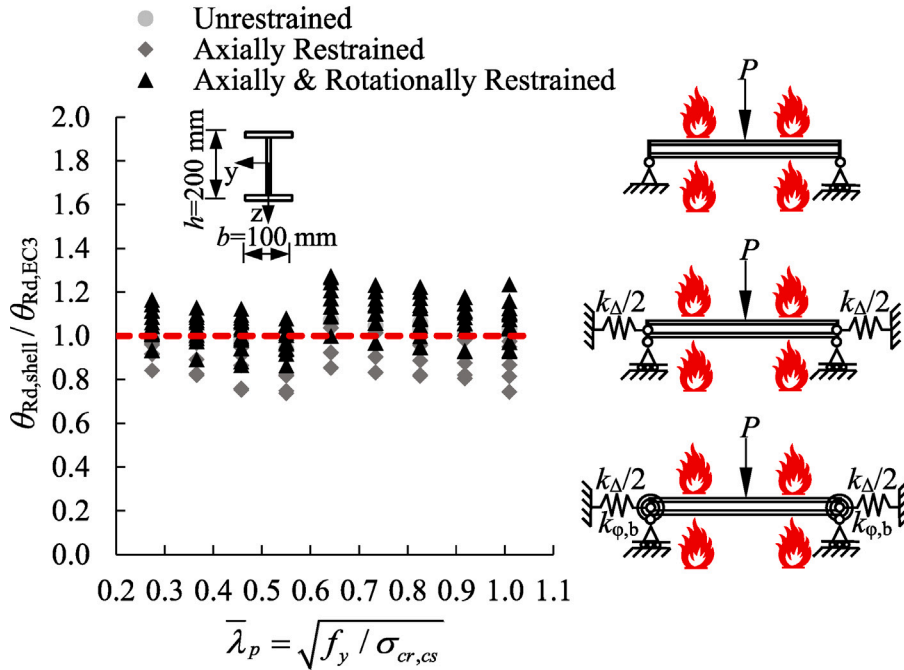
and Young’s modulus reduction factors and (v) β values ranging between 0 and 1 (i.e. $\beta = 0-1$) which are used to modify the proportion of the applied axial compression force and bending moment, thereby considering varying degrees of axial compression and bending moment intensities. Grade S355 steel was used in the parametric studies. It should also be noted that in both shell finite element analyses and the application of the proposed fire design approach with beam finite element models, the steel beam–columns were loaded proportionally by increasing the load factor α which led to the increase of the applied axial compression N_{Ed} and bending moments M_{Ed} at the same rate.

Figs. 14–16 show the ultimate resistance predictions for hot-rolled and welded steel beam–columns subjected to combined axial compression and bending with elevated temperature member slendernesses λ_θ of 0.5, 1.0 and 1.5 (i.e. $\lambda_\theta = 0.5, 1.0, 1.5$). The figures compare

(i) the maximum applied axial force N_{Ed} normalised by the product of the cross-sectional area A , the elevated temperature yield strength reduction factor $k_{y,\theta}$ and the yield strength f_y (i.e. $N_{Ed}/(Ak_{y,\theta}f_y)$) against (ii) the maximum applied bending moment M_{Ed} normalised by the product of the plastic section modulus W_{pl} , the yield strength reduction factor $k_{y,\theta}$ and the yield strength f_y (i.e. $M_{Ed}/(W_{pl}k_{y,\theta}f_y)$). For the case of the ultimate strengths determined using the proposed fire design approach, a distinction is made between steel beam–columns where the peak load or the strain limit governed the capacity. In addition to the results presented in Figs. 14–16, Table 8 shows the ratios of the ultimate load factors obtained from the benchmark shell finite element models $\alpha_{Rd,\theta,shell}$ to those determined using the proposed method $\alpha_{Rd,\theta,prop}$ (i.e. $\alpha_{Rd,\theta,shell}/\alpha_{Rd,\theta,prop}$) for all the considered cases shown in Table 7. Note that an $\alpha_{Rd,\theta,shell}/\alpha_{Rd,\theta,prop}$ ratio is calculated as



(a) Proposed method



(b) EN 1993-1-2 [6]

Fig. 13. Comparison of the accuracy of the proposed method against EN 1993-1-2 [6] for steel beams analysed adopting the anisothermal analysis technique.

$$\frac{\alpha_{Rd,\theta,shell}}{\alpha_{Rd,\theta,prop}} = \frac{N_{Ed,shell}}{N_{Ed,prop}} = \frac{M_{Ed,shell}}{M_{Ed,prop}} \quad (16)$$

where $N_{Ed,shell}$ and $M_{Ed,shell}$ are the maximum values of the applied axial compression and bending moment obtained from a shell finite element model and $N_{Ed,prop}$ and $M_{Ed,prop}$ are the maximum values of the applied axial compression and bending moment determined through the proposed GMNIA with strain limits approach implemented using a

beam finite element model; since the beam–columns were loaded proportionally, $N_{Ed,shell}/N_{Ed,prop}$ and $M_{Ed,shell}/M_{Ed,prop}$ ratios are identical (i.e. $\alpha_{Rd,\theta,shell}/\alpha_{Rd,\theta,prop} = N_{Ed,shell}/N_{Ed,prop} = M_{Ed,shell}/M_{Ed,prop}$). Additionally, the ratios of the ultimate load factors obtained from the benchmark shell finite element models $\alpha_{Rd,\theta,shell}$ to those determined using the EN 1993-1-2 [6] design provisions $\alpha_{Rd,\theta,EC3}$ (i.e. $\alpha_{Rd,\theta,shell}/\alpha_{Rd,\theta,EC3}$) are also shown in Table 8 for comparison where $\alpha_{Rd,\theta,shell}/\alpha_{Rd,\theta,EC3}$ ratios are determined through Eq. (16) but using the ultimate values of axial compression $N_{Ed,EC3}$ and bending moment

Table 7

Parameters used in the investigation of the accuracy of the proposed design approach for steel beam–columns analysed adopting the isothermal analysis approach.

Loading conditions	Cross-section (<i>h/b</i>)	Fabrication process	θ	$\bar{\lambda}_\theta$	β
	IPE 300 (2.00)	Hot-rolled Welded	300 °C 500 °C 700 °C	0.5 1.0 1.5	0.0-1.0
	HEB 300 (1.00)				
	HEAA 300 (0.94)				

Table 8

Capacity predictions achieved using the proposed method and EN 1993-1-2 [6] compared with benchmark shell finite element model predictions for hot-rolled and welded I-section steel beam–columns at elevated temperatures tested under in-plane bending with isothermal conditions.

Type	θ (°C)	<i>N</i>	$\alpha_{Rd,\theta,shell} / \alpha_{Rd,\theta,EC3}$				$\alpha_{Rd,\theta,shell} / \alpha_{Rd,\theta,prop}$			
			Mean	CoV	Max	Min	Mean	CoV	Max	Min
Uniform moment (major)	300, 500,	594	1.25	0.215	1.94	0.86	1.04	0.048	1.36	0.95
Uniform moment (minor)		594	1.43	0.214	2.42	0.82	1.05	0.063	1.32	0.92
Nonuniform moment (major)	700	594	1.21	0.227	1.94	0.75	1.05	0.058	1.44	0.93
Total		1782	1.30	0.231	2.42	0.75	1.05	0.057	1.44	0.92

resistances $M_{Ed,EC3}$ calculated using EN 1993-1-2 [6] provisions in lieu of $N_{Ed,prop}$ and $M_{Ed,prop}$. Figs. 14, 15, 16 and Table 8 demonstrate that the proposed fire design method provides considerably more accurate ultimate resistance predictions for steel beam–columns relative to EN 1993-1-2 [6].

5.2. Anisothermal analysis technique

Table 9 summarises the parametric study performed for the verification of the proposed fire design method for steel beam–columns when it is applied using the anisothermal analysis technique. The parametric study comprised (i) hot-rolled IPE 300 sections, (ii) three room temperature slendernesses $\bar{\lambda}$ for flexural buckling about the corresponding bending axis which are equal to 0.5, 1.0 and 1.5 (i.e. $\bar{\lambda} = 0.5, 1.0$ and 1.5), (iii) a combined axial compression and bending intensity α_{N-M} of 0.50 (i.e. $\alpha_{N-M} = 0.50$) and (iv) β values of 0, 0.2, 0.4, 0.6, 0.8 and 1.0 which are used to modify the proportion of the axial compression force N_{Ed} and bending moment M_{Ed} (i.e. $\beta = 0, 0.2, 0.4, 0.6, 0.8$ and 1.0) such that the applied axial compression N_{Ed} is equal to

$$N_{Ed} = \alpha_{N-M}(1 - \beta)N_{pl} = \alpha_{N-M}(1 - \beta)Af_y \quad (17)$$

where A is the cross-section area and N_{pl} is the room temperature cross-section axial force resistance and the applied bending moment M_{Ed} is equal to

$$M_{Ed} = \alpha_{N-M}\beta M_{pl} = \alpha_{N-M}\beta W_{pl}f_y \quad (18)$$

in which W_{pl} is the plastic section modulus with respect to the corresponding bending axis and M_{pl} is the room temperature cross-section plastic bending moment resistance. Thus, $\beta = 0$ corresponds to pure axial compression and $\beta = 1.0$ corresponds to pure bending moment.

As can be seen from Table 9, the parametric study also comprised (i) axially and rotationally unrestrained beam–columns, (ii) axially restrained beam–columns with axial restraint ratios α_Δ of 0.02, 0.05 and 0.10 (i.e. $\alpha_\Delta = k_\Delta/(EA/L) = 0.02, 0.05$ and 0.10) and (iii) axially and rotationally restrained beam–columns with a rotational restraint ratio $\alpha_{\varphi,c}$ equal to 0.50 (i.e. $\alpha_{\varphi,c} = k_{\varphi,c}/(4EI/L) = 0.50$) and axial restraint ratios α_Δ of 0.02, 0.05 and 0.10 (i.e. $\alpha_\Delta = k_\Delta/(EA/L) = 0.02, 0.05$ and 0.10). The restraint ratios were selected in order to capture the typical values which occur in real buildings [70] and the beam–columns were subjected to major axis bending.

Fig. 17 shows the limit temperature θ_{Rd} predictions obtained using the shell finite element models and proposed fire design approach versus the cross-section slendernesses $\bar{\lambda}_p$ for unrestrained, axially restrained and axially and rotationally restrained IPE 300 beam–columns. As can be seen from Fig. 17, the proposed GMNIA with strain limits based fire design approach furnishes quite accurate and safe-sided limit temperature θ_{Rd} predictions for steel beam–columns analysed using the anisothermal analysis technique. Additionally, Table 10 shows the ratios of the limit temperatures θ_{Rd} from the benchmark shell finite element models $\theta_{Rd,shell}$ to those determined through the proposed fire design approach $\theta_{Rd,prop}$ (i.e. $\theta_{Rd,shell}/\theta_{Rd,prop}$) and EN 1993-1-2 [6] $\theta_{Rd,EC3}$ (i.e. $\theta_{Rd,shell}/\theta_{Rd,EC3}$) for all the considered unrestrained, axially restrained and axially and rotationally restrained steel beam–columns (see Table 9). Fig. 18 also illustrates the $\theta_{Rd,shell}/\theta_{Rd,prop}$ and $\theta_{Rd,shell}/\theta_{Rd,EC3}$ ratios from Table 10 whereby the accuracy of the proposed fire design method can be visually compared to that of EN 1993-1-2 [6]. As can be seen from Table 10 and Fig. 18, the proposed GMNIA with strain limits fire design approach provides considerably more accurate as well as safer limit temperature predictions compared to those determined using EN 1993-1-2 [6].

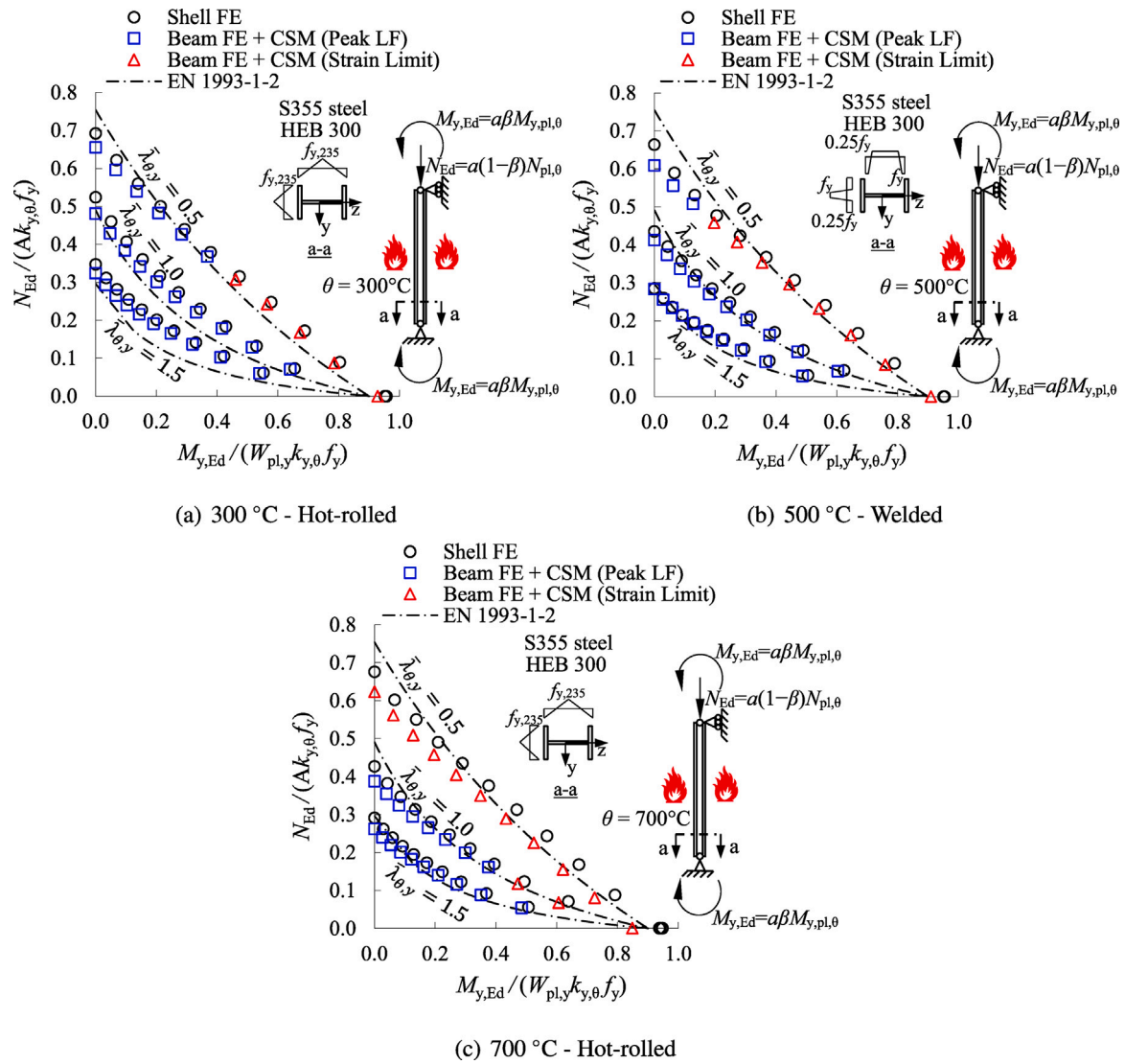


Fig. 14. Capacity predictions achieved using the proposed method and shell finite element models for hot-rolled and welded HEB 300 steel beam-columns analysed adopting the isothermal analysis method.

6. Reliability analysis

The reliability of the proposed fire design method and that of EN 1993-1-2 [6] is assessed in Table 11 for the fire design of steel beams and beam-columns by adopting the three reliability criteria proposed by Kruppa [71]. All of the results from the parametric studies described in Sections 4.1, 4.2, 5.1 and 5.2 are considered within the reliability analysis. Criterion 1 of Kruppa [71] states that none of the ultimate resistance predictions from a design method R_{method} should exceed those attained using the GMNIA of the shell finite element models R_{GMNIA} by more than 15% (i.e. $(R_{method} - R_{GMNIA})/R_{GMNIA} \leq 15\%$). Criterion 2 of Kruppa [71] indicates that the number of the ultimate resistance predictions of a design method R_{method} that are greater than the GMNIA predictions R_{GMNIA} must be less than 20% of all the considered cases (i.e. $num(R_{method} > R_{GMNIA})/num(R_{GMNIA}) \leq 20\%$). Criterion 3 of Kruppa [71] states that on average the ultimate resistance predictions from a design method R_{method} need to be less than those determined through the GMNIA of the shell finite element models R_{GMNIA} (i.e. $\bar{X}[(R_{method} - R_{GMNIA})/R_{GMNIA}] \leq 0\%$). In Table 11, the percentage of the design predictions R_{method} greater than the GMNIA predictions R_{GMNIA} by more than 15% is shown under Criterion 1, the percentage of the unsafe design predictions for which the predictions from the design method R_{method} are greater than those achieved through

the GMNIA of the shell finite element models R_{GMNIA} (i.e. $R_{method} > R_{GMNIA}$) is shown under Criterion 2 and the average percentage differences between the GMNIA predictions R_{GMNIA} and the predictions from the design method R_{method} are shown under Criterion 3 where negative percentages signify that the capacity predictions are safe-sided on average. Table 11 shows that the proposed fire design method fulfils all the three reliability criteria of Kruppa [71]. By contrast, the design predictions of EN 1993-1-2 [6] fail to satisfy the reliability criteria of Kruppa [71] in a large number of cases, thus indicating that the proposed method leads to a greater degree of reliability compared to EN 1993-1-2 [6] for the fire design of steel beams and beam-columns.

7. Summary of the proposed design method using worked examples

In this section the application of the proposed design method is summarised using two worked examples. Worked example 1 considers a steel beam-column analysed using the isothermal analysis technique and worked example 2 considers a restrained steel beam analysed using the anisothermal analysis technique.

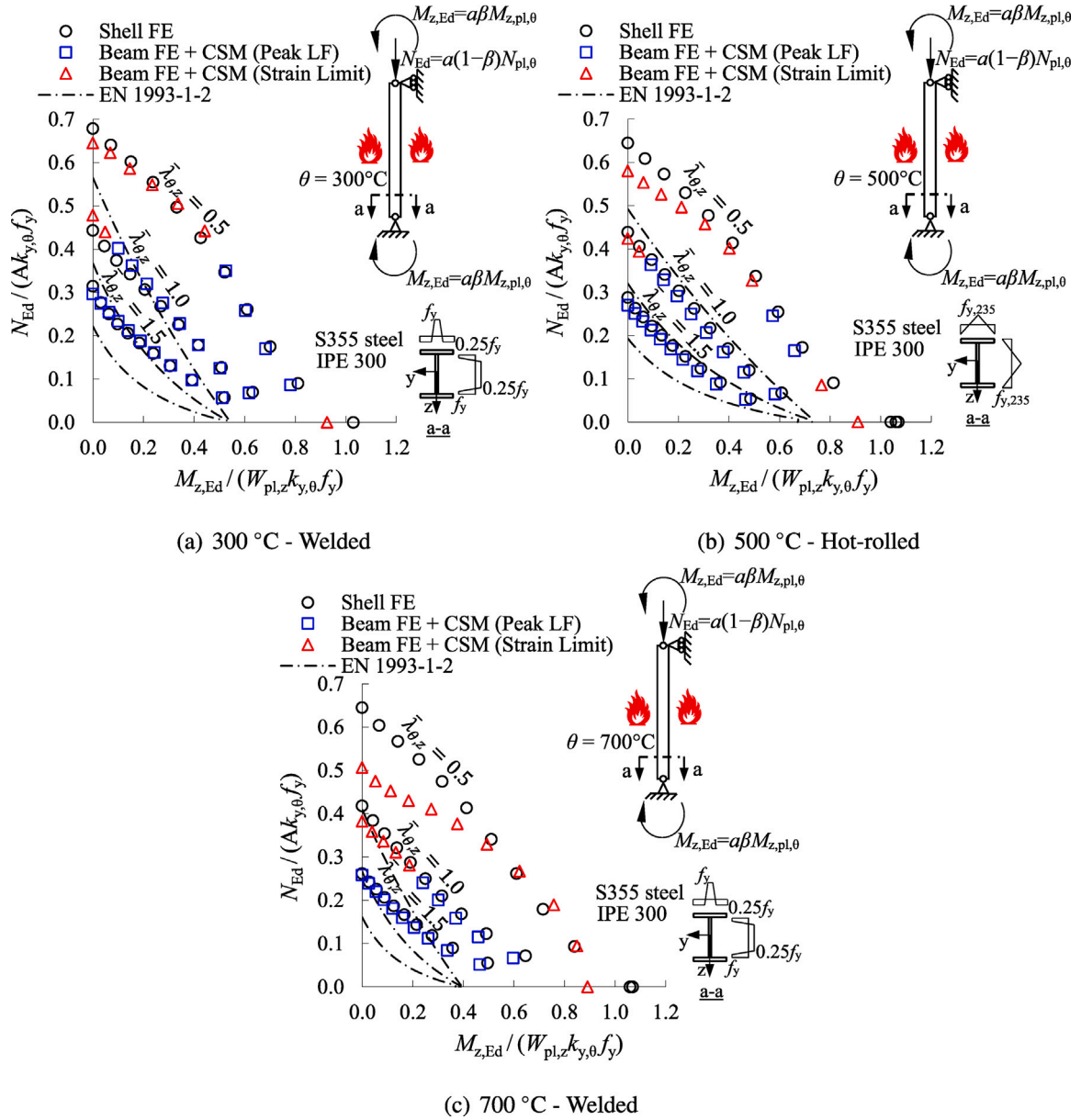


Fig. 15. Capacity predictions achieved using the proposed method and shell finite element models for hot-rolled and welded IPE 300 steel beam-columns analysed adopting the isothermal analysis method.

7.1. Worked example 1

Worked example 1 shown in Fig. 19 considers a grade S355 steel ($f_y = 355 \text{ N/mm}^2$) HEB 300 beam-column subjected to a combined design axial load N_{Ed} of 278.34 kN (i.e. $N_{Ed} = 278.34 \text{ kN}$) and uniform design major axis moment $M_{y,Ed}$ of 314.05 kNm (i.e. $M_{y,Ed} = 314.05 \text{ kNm}$) at a temperature θ of 500 °C. The beam-column is analysed using the isothermal analysis approach.

7.1.1. Calculation of the full cross-section elastic local buckling stress $\sigma_{cr,cs}$

The method recommended in [20] is used herein to calculate $\sigma_{cr,cs}$. The corresponding elastic buckling stresses with simply-supported boundary conditions σ_{cr}^{SS} are 1309.45 MPa for the flange plate (i.e. $\sigma_{cr,f}^{SS} = 1309.45 \text{ MPa}$) and 5429.70 MPa for the web plate (i.e. $\sigma_{cr,w}^{SS} = 5429.70 \text{ MPa}$); and the elastic buckling stresses with fixed boundary conditions σ_{cr}^F are 3806.55 MPa for the flange plate (i.e. $\sigma_{cr,f}^F = 3806.55 \text{ MPa}$) and 9131.25 MPa for the web plate (i.e. $\sigma_{cr,w}^F = 9131.25 \text{ MPa}$). Since the beam-column cross-section is an I-section

subjected to major axis bending plus axial compression, the flange load correction factor β_f and the web load correction factor β_w are equal to one (i.e. $\beta_f = 1$ and $\beta_w = 1$). The governing ratio ϕ is calculated as:

$$\phi = \frac{\beta_f \sigma_{cr,f}^{SS}}{\beta_w \sigma_{cr,w}^{SS}} = 0.24$$

Since $\phi < 1$, the flange plate is deemed critical. The lower and upper bounds to the full cross-section local buckling stress are as follows:

$$\sigma_{cr,p}^{SS} = \min(\beta_f \sigma_{cr,f}^{SS}, \beta_w \sigma_{cr,w}^{SS}) = 1309.45 \text{ MPa}$$

$$\sigma_{cr,p}^F = \min(\beta_f \sigma_{cr,f}^F, \beta_w \sigma_{cr,w}^F) = 3806.45 \text{ MPa}$$

The interaction coefficient ξ for an I-section subjected to compression and major axis bending is given by:

$$\xi = 0.15 \frac{t_f}{t_w} \phi \geq \frac{t_w}{t_f} (0.4 - 0.25\phi) = 0.197$$

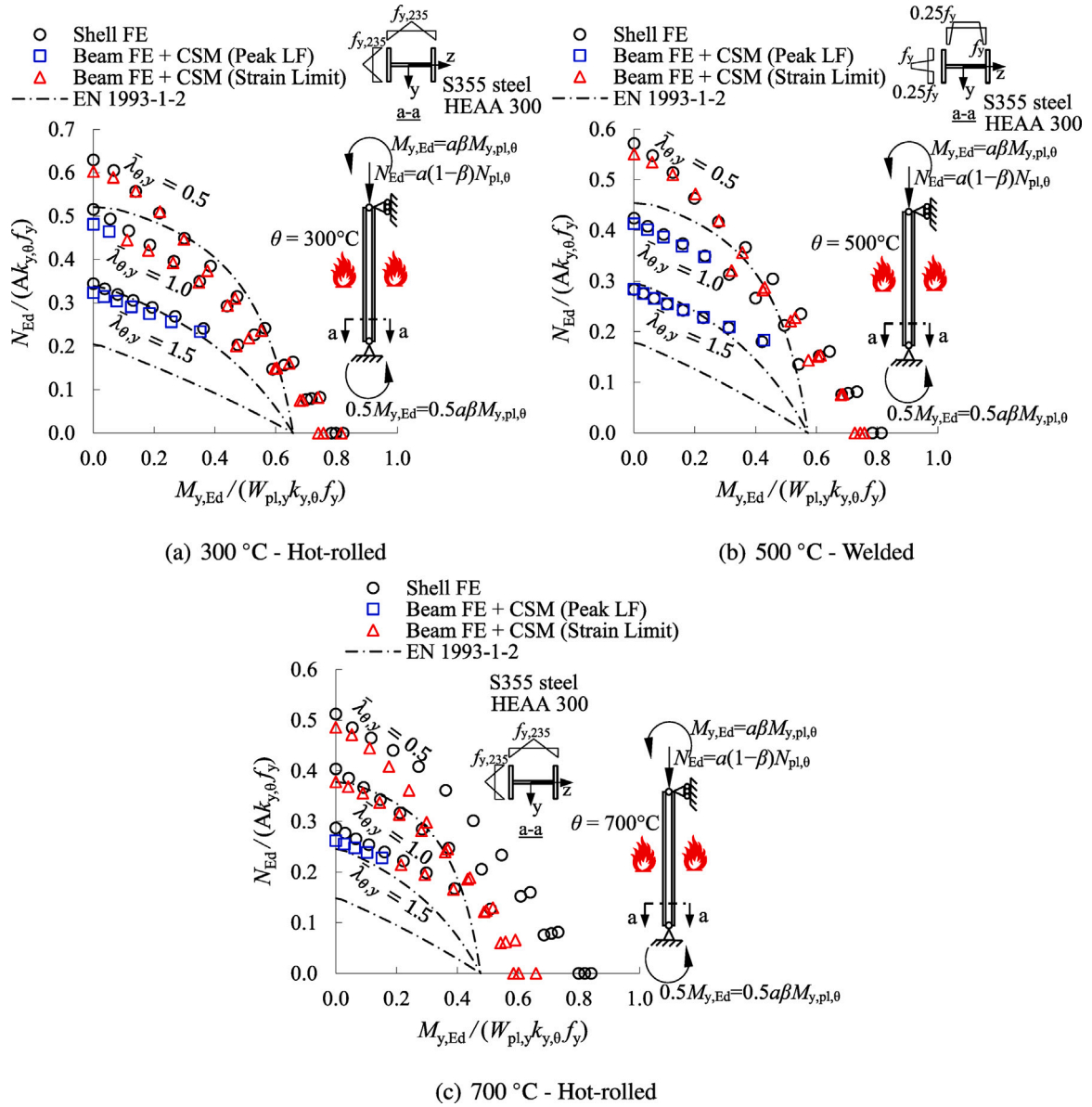


Fig. 16. Capacity predictions achieved using the proposed method and shell finite element models for hot-rolled and welded HEAA 300 steel beam–columns analysed adopting the isothermal analysis method.

The full cross-section elastic local buckling stress $\sigma_{cr,cs}$ is then calculated as:

$$\sigma_{cr,cs} = \sigma_{cr,p}^{SS} + \xi(\sigma_{cr,p}^F - \sigma_{cr,p}^{SS}) = 1309.45 + 0.197(3806.45 - 1309.45) = 1800.56 \text{ MPa}$$

Note that the full cross-section local buckling stress $\sigma_{cr,cs}$ determined using the finite strip analysis software CUFSM [21] is equal to 1786.70 MPa for the considered cross-section and loading type.

7.1.2. Calculation of the elevated temperature cross-section slenderness $\bar{\lambda}_{p,\theta}$

The elevated temperature cross-section slenderness $\bar{\lambda}_{p,\theta}$ is calculated using the room temperature cross-section slenderness $\bar{\lambda}_p$, the 0.2% proof strength reduction factor $k_{p0.2,\theta}$ equal to 0.56 at 500 °C (i.e. $k_{p0.2,\theta} = 0.56$) and the elastic modulus reduction factor $k_{E,\theta}$ equal to 0.60 at 500 °C (i.e. $k_{E,\theta} = 0.60$).

$$\bar{\lambda}_{p,\theta} = \bar{\lambda}_p \sqrt{\frac{k_{p0.2,\theta}}{k_{E,\theta}}} = \sqrt{\frac{f_y}{\sigma_{cr,cs}}} \sqrt{\frac{k_{p0.2,\theta}}{k_{E,\theta}}} = \sqrt{\frac{355.00}{1800.56}} \sqrt{\frac{0.56}{0.60}} = 0.43$$

7.1.3. Calculation of the elevated temperature CSM strain limit $\epsilon_{csm,\theta}$

$\epsilon_{csm,\theta}$ is determined using the elevated temperature base curve. Since $\bar{\lambda}_{p,\theta} < 0.68$, the cross-section is considered non-slender and therefore $\epsilon_{csm,\theta}/\epsilon_{y,\theta}$ is determined as:

$$\epsilon_{csm,\theta}/\epsilon_{y,\theta} = \frac{0.25}{\bar{\lambda}_{p,\theta}^{-3.6}} + \frac{0.002}{\epsilon_{y,\theta}} \leq \left(\Omega, \frac{C_1}{\epsilon_{y,\theta}} \right) = 6.57$$

where the upper limit Ω is set to 15 (i.e. $\Omega = 15$), the upper limit C_1 is equal to 0.02 (i.e. $C_1 = 0.02$) and the elevated temperature yield strain $\epsilon_{y,\theta}$ is equal to 0.00157 (i.e. $\epsilon_{y,\theta} = 0.00157$). $\epsilon_{csm,\theta}$ is then calculated as:

$$\epsilon_{csm,\theta} = 6.57 \epsilon_{y,\theta} = 6.57 \times 0.00157 = 0.0103$$

7.1.4. GMNIA using beam finite elements adopting the isothermal approach

GMNIA is performed using 101 beam finite elements to discretise the beam–column over its 4360.52 mm length. The model uses equivalent geometric imperfections with a magnitude equal to:

$$e_0 = \alpha \beta L \geq L/1000 = 0.53 \times (1/250) \times 4360.52 \geq 4360.52/1000 = 9.22 \text{ mm}$$

Table 9

Parameters used in the investigation of the accuracy of the proposed fire design approach for steel beam–columns analysed using the anisothermal analysis method.

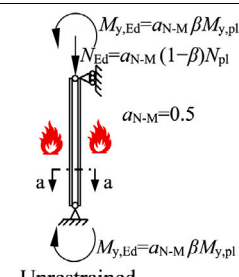
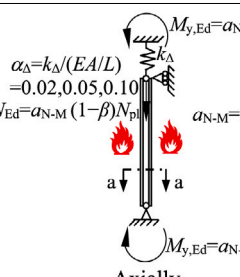
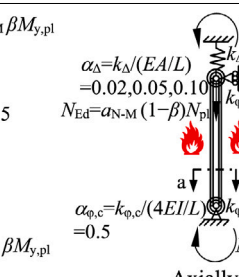
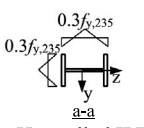
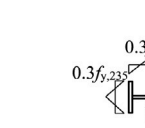

End restraint types & stiffnesses, cross-section and loading conditions			$\bar{\lambda}$	β
 <p>Unrestrained</p>	 <p>Axially restrained</p>	 <p>Axially & rotationally restrained</p>	0.0	0.2
			0.50	0.6
 <p>Hot-rolled IPE 300 section</p>	 <p>Hot-rolled IPE 300 section</p>	 <p>Hot-rolled IPE 300 section</p>	1.00	0.8
			1.50	1.0

Table 10

Comparison of the critical temperature predictions obtained through the proposed method and EN 1993-1-2 [6] against those determined using the benchmark shell finite element models for hot-rolled steel IPE 300 beam–columns in fire analysed adopting the anisothermal analysis method.

Boundary conditions	N	$\theta_{Rd,shell} / \theta_{Rd,EC3}$				$\theta_{Rd,shell} / \theta_{Rd,prop}$			
		Mean	CoV	Max	Min	Mean	CoV	Max	Min
Unrestrained	18	1.30	0.260	1.92	0.84	1.04	0.026	1.11	1.01
Axially restrained	54	1.01	0.245	1.52	0.52	1.06	0.079	1.34	0.92
Axially & Rotationally restrained	54	1.45	0.190	2.13	0.89	1.09	0.098	1.48	0.95
Total	126	1.24	0.276	2.13	0.52	1.07	0.086	1.48	0.92

Table 11

Reliability of the proposed method and EN 1993-1-2 [6] for the assessment of steel beams and beam–columns in fire on the basis of the reliability criteria defined by Kruppa [71].

Type	Criterion 1	Criterion 2	Criterion 3	
Proposed method	Beam (Isothermal)	0.00	19.92	−8.42
	Beam (Anisothermal)	0.00	19.83	−6.36
	Beam–column (Isothermal)	0.00	14.81	−4.20
	Beam–column (Anisothermal)	0.00	14.29	−5.82
EN 1993-1-2 [6]	Beam (Isothermal)	6.31 ^a	22.58 ^a	−10.39
	Beam (Anisothermal)	11.64 ^a	39.22 ^a	−0.91
	Beam–column (Isothermal)	2.08 ^a	15.71	−18.99
	Beam–column (Anisothermal)	15.08 ^a	26.19 ^a	−12.32

^a Indicates the corresponding criterion has been violated.

where the imperfection factor α is calculated as $0.65 \sqrt{235/f_y}$ and the reference bow imperfection β is equal to $1/250$ (i.e. $\beta = 1/250$). The analysis is completed by first increasing the temperature to 500 °C followed by the application of a proportionally increasing axial load and end-moments using the modified Riks method. Fig. 20 shows the applied load versus the compressive strain at the critical cross-section. As can be seen in Fig. 20, the strain limit is obtained at a load factor $\alpha_{csm,\theta}$ of 1.20 prior to the peak load factor $\alpha_{peak,\theta}$ of 1.25, therefore the capacity of the beam–column is governed by the strain limit.

7.1.5. Resistance verification against applied load

The characteristic resistance load factor $\alpha_{Rk,\theta}$ of the beam–column at 500 °C is equal to 1.20 corresponding to the axial load and moment at which the critical strain in the cross-section first reaches the strain

limit $\alpha_{csm,\theta}$ (i.e. $\alpha_{Rk,\theta} = \alpha_{csm,\theta}$). Dividing $\alpha_{Rk,\theta}$ by the partial factor for resistance in fire conditions $\gamma_{M,fi}$ which is equal to 1.00 (i.e. $\gamma_{M,fi} = 1.00$), the design resistance is given by:

$$\alpha_{Rd,\theta} = \frac{\alpha_{Rk,\theta}}{\gamma_{M,fi}} = \frac{1.20}{1.00} \geq 1.00 \quad \therefore \text{Pass}$$

Therefore, the beam–column is deemed satisfactory at 500 °C. Note that the design resistance load factor $\alpha_{Rd,\theta}$ determined through the benchmark shell finite element model is 1.24. Moreover, it should be noted that when the anisothermal analysis technique is adopted for the considered design problem where the member is first loaded and then heated up to failure, the design load factor $\alpha_{Rd,\theta}$ of 1.20 results in a limit temperature θ_{Rd} of 500 °C. This demonstrates that the anisothermal and isothermal analysis techniques provide very similar

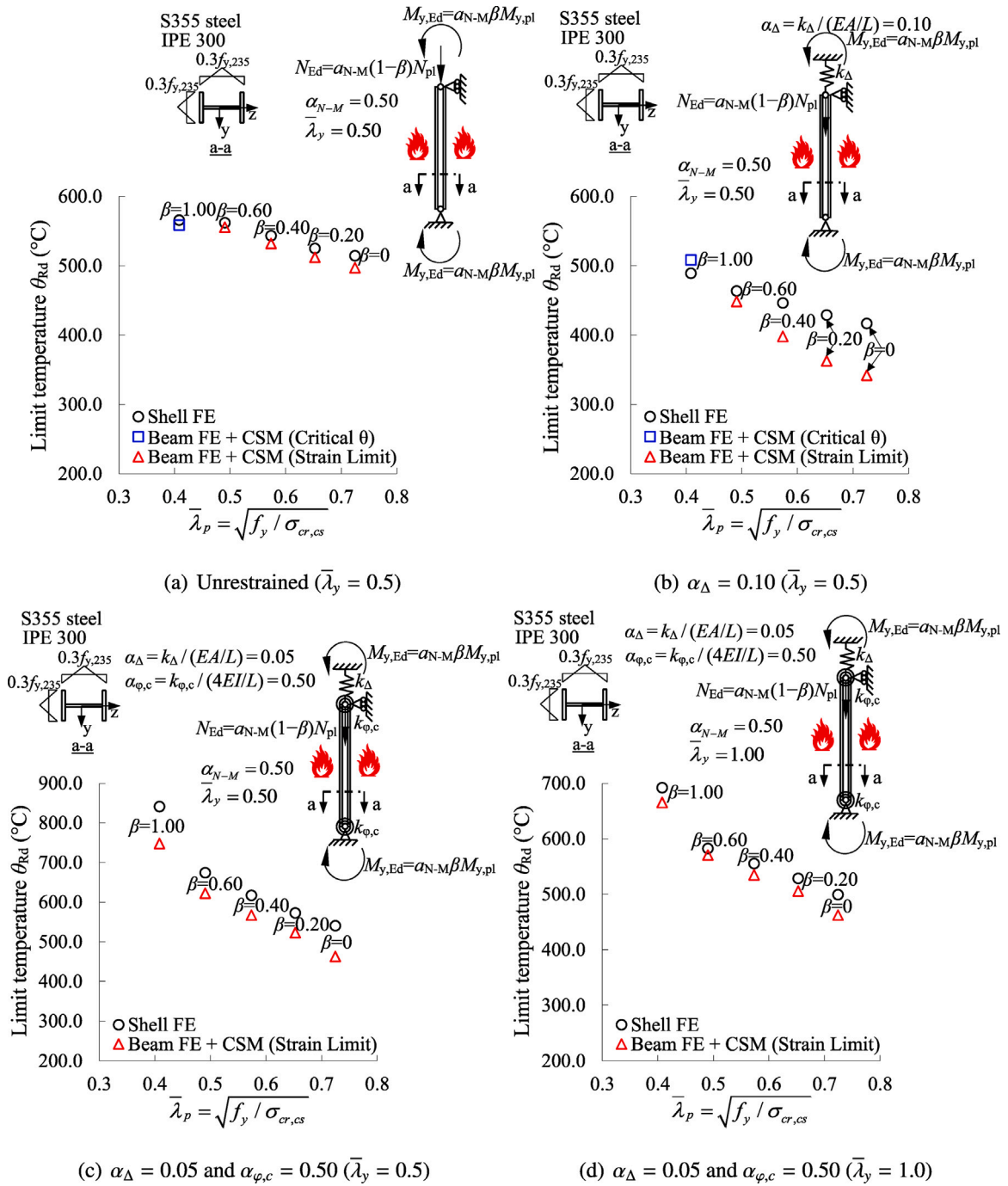


Fig. 17. Capacity predictions of the proposed method and benchmark shell finite element models for hot-rolled IPE 300 steel beam-columns analysed using the anisothermal analysis method.

predictions, though the former represents the actual behaviour of a steel member in fire more realistically while the latter directly provides ultimate load carrying capacities at certain elevated temperature values.

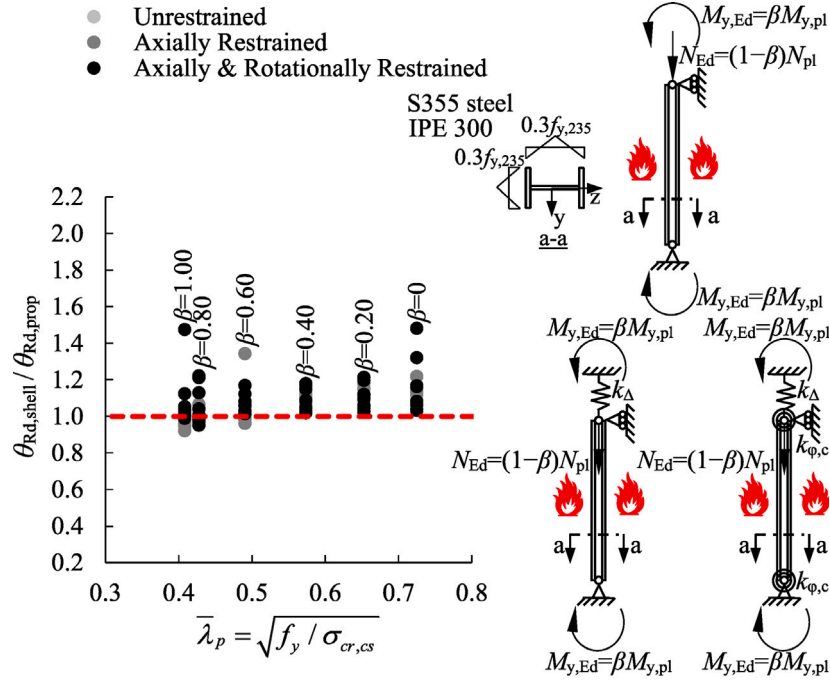
7.2. Worked example 2

Worked example 2 shown in Fig. 21 considers a grade S355 steel ($f_y = 355 \text{ N/mm}^2$) IPE 300 beam under 3-point bending. The design value of the central load P is 69.18 kN (i.e. $P = 69.18 \text{ kN}$) which corresponds to a design moment $M_{y,Ed}$ of 106.87 kNm (i.e. $M_{y,Ed} = PL/4 = 106.87 \text{ kNm}$). The beam is required to withstand a design temperature θ_{Ed} of 550 °C and is analysed using the anisothermal

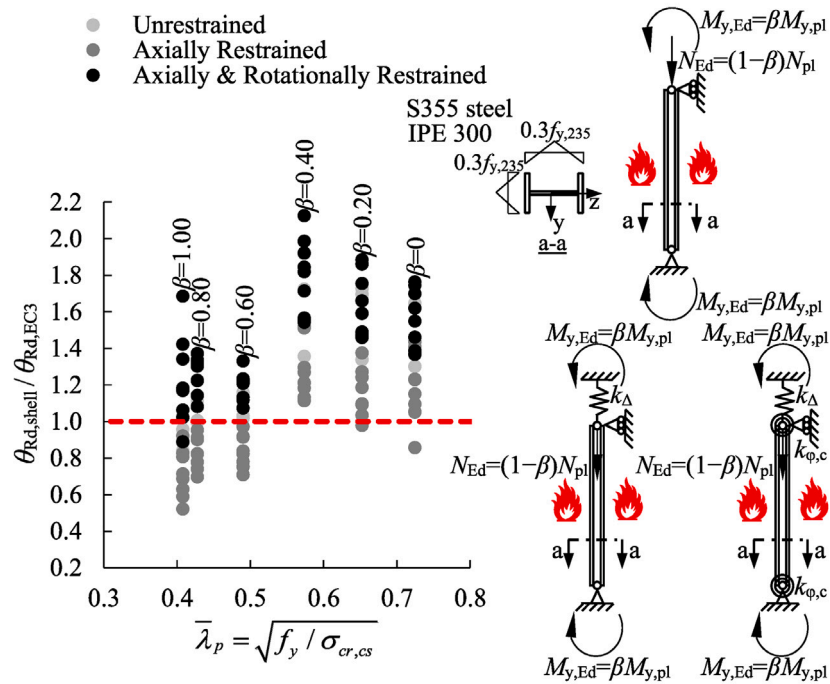
analysis approach. The beam has axial end-restraint k_{Δ} equivalent to 17.63 kN/mm (i.e. $k_{\Delta} = 17.63 \text{ kN/mm}$) where k_{Δ} is equal to the axial restraint stiffness ratio $\alpha_{\Delta} = 0.1$ multiplied by the axial stiffness of the beam $k_{\Delta} = \alpha_{\Delta} k_{\Delta} = 0.1 k_{\Delta}$). In addition, the beam has rotational end-restraints $k_{\phi,b}$ at both ends equal to 1359.21 kNm/rad (i.e. $k_{\phi,b} = 1359.21 \text{ kNm/rad}$) where $k_{\phi,b}$ is equal to the rotational restraint stiffness ratio $\alpha_{\phi,b}$ of 0.5 multiplied by the rotational stiffness of the beam $k_{\phi,b} = \alpha_{\phi,b} k_{\phi,b} = 0.5 k_{\phi,b}$.

7.2.1. Calculation of the full cross-section elastic local buckling stress $\sigma_{cr,cs}$

The method recommended in [20] is used in this section to calculate $\sigma_{cr,cs}$. The corresponding elastic buckling stresses with simply-supported boundary conditions σ_{cr}^{SS} are 1661.15 MPa for the flange



(a) Proposed method



(b) EN 1993-1-2 [6]

Fig. 18. Comparison of the accuracy of the proposed fire design method against EN 1993-1-2 [6] for steel beam–columns analysed using the anisothermal analysis approach.

HEB 300

$$\bar{\lambda}_{p,0} = 0.43 \text{ (Class 3)}$$

$$L = 4360.52 \text{ mm } (\bar{\lambda}_{\theta} = 0.5)$$

S355 Steel - 500 °C (EN 1993-1-2):

$$f_{p0.2,\theta} = 198.00 \text{ N/mm}^2$$

$$f_{2.0,\theta} = 276.90 \text{ N/mm}^2$$

$$E_{\theta} = 126000.00 \text{ N/mm}^2$$

$$n_{\theta} = 8.52$$

$$N_{Ed} = 278.34 \text{ kN}$$

$$M_{y,Ed} = 314.05 \text{ kNm}$$

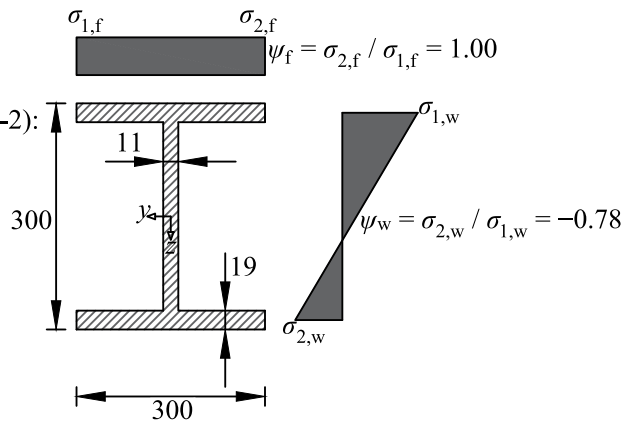


Fig. 19. Worked example 1: HEB 300 beam-column. All dimensions are in mm. Not to scale.

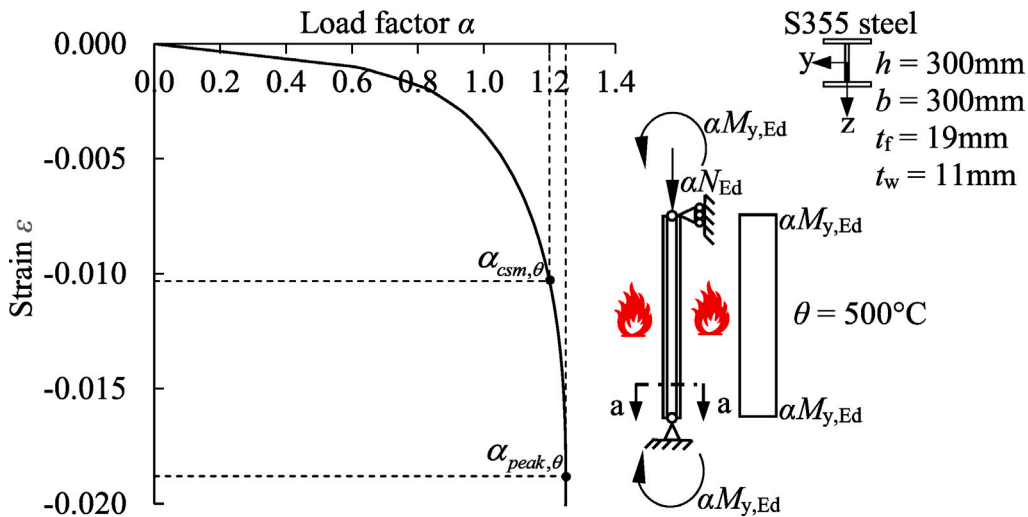


Fig. 20. Load factor versus the compressive strain at the critical cross-section of the HEB 300 beam-column.

IPE 300

$$\bar{\lambda}_p = 0.41 \text{ (Class 3)}$$

$$L = 6179.26 \text{ mm}$$

$$k_{\Delta} = 17.63 \text{ kN/mm}$$

$$k_{\phi,b} = 1359213.69 \text{ kNm}$$

S355 Steel

$$P = 69.18 \text{ kN} \text{ \& } \theta_{Ed} = 550 \text{ }^{\circ}\text{C}$$

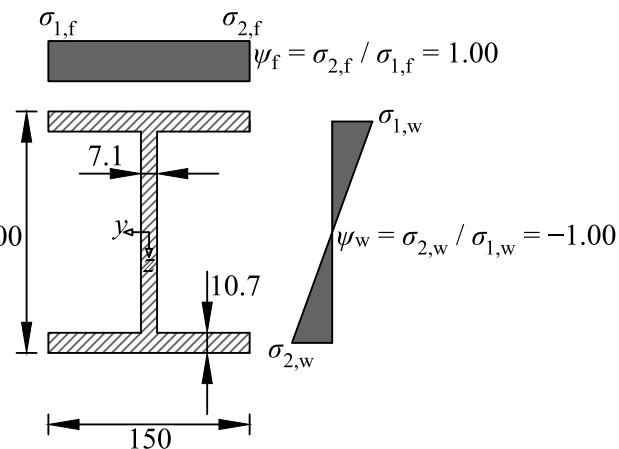


Fig. 21. Worked example 2: IPE 300 beam. All dimensions are in mm. Not to scale.

plate (i.e. $\sigma_{cr,f}^{SS} = 1661.15 \text{ MPa}$) and 2732.21 MPa for the web plate (i.e. $\sigma_{cr,w}^{SS} = 2732.21 \text{ MPa}$); and the elastic buckling stresses with fixed boundary conditions σ_{cr}^F are 4828.94 MPa for the flange plate (i.e. $\sigma_{cr,f}^F = 4828.94 \text{ MPa}$) and 4527.01 MPa for the web plate (i.e. $\sigma_{cr,w}^F = 4527.01 \text{ MPa}$). Since the beam section is an I-section subjected to major

axis bending, the flange load correction factor β_f and the web load correction factor β_w are equal to one (i.e. $\beta_f = 1$ and $\beta_w = 1$). The governing ratio ϕ is calculated as:

$$\phi = \frac{\beta_f \sigma_{cr,f}^{SS}}{\beta_w \sigma_{cr,w}^{SS}} = 0.61$$

Since $\phi < 1$, the flange plate is deemed critical. The lower and upper bounds to the full cross-section local buckling stress are as follows:

$$\sigma_{cr,p}^{SS} = \min(\beta_f \sigma_{cr,f}^{SS}, \beta_w \sigma_{cr,w}^{SS}) = 1661.15 \text{ MPa}$$

$$\sigma_{cr,p}^F = \min(\beta_f \sigma_{cr,f}^F, \beta_w \sigma_{cr,w}^F) = 4527.01 \text{ MPa}$$

The interaction coefficient ξ for a I-section subject to major axis bending is given by:

$$\xi = 0.15 \frac{t_f}{t_w} \phi \geq \frac{t_w}{t_f} (0.4 - 0.25\phi) = 0.165$$

The full cross-section elastic local buckling stress $\sigma_{cr,cs}$ is then calculated as:

$$\begin{aligned} \sigma_{cr,cs} &= \sigma_{cr,p}^{SS} + \xi(\sigma_{cr,p}^F - \sigma_{cr,p}^{SS}) = 1661.15 + 0.165(4527.01 - 1661.15) \\ &= 2132.77 \text{ MPa} \end{aligned}$$

Note that the full cross-section local buckling stress $\sigma_{cr,cs}$ determined using the finite strip analysis software CUFSM [21] is equal to 2094.64 MPa for the considered cross-section and loading type.

7.2.2. Calculation of local buckling half-wavelength $L_{b,cs}$

The local buckling half-wavelength of the full cross-section of the beam $L_{b,cs}$ is determined in accordance with the procedure put forward in [39]. The elastic local buckling half-wavelengths for simply-supported boundary conditions L_b^{SS} are determined as 345.63 mm for the flange plate (i.e. $L_{b,f}^{SS} = 345.63$ mm) and 193.83 mm for the web plate (i.e. $L_{b,w}^{SS} = 193.83$ mm); and the elastic local buckling half-wavelengths for fixed boundary conditions L_b^F are determined as 123.75 mm for the flange plate (i.e. $L_{b,f}^F = 123.75$ mm) and 135.97 mm for the web plate (i.e. $L_{b,w}^F = 135.97$ mm). The transition function η for an I-section subjected to major axis bending is determined using the governing ratio of $\phi = 0.61$ which was calculated previously in the determination of $\sigma_{cr,cs}$:

$$\eta = 1 - \frac{1}{(\phi - 0.5)^3 + 1} \geq 0 = 1 - \frac{1}{(0.61 - 0.5)^3 + 1} = 0.001$$

The lower and upper bounds to the full cross-section local buckling half-wavelength are as follows:

$$L_{b,p}^{SS} = L_{b,w}^{SS} \eta + L_{b,f}^{SS} (1 - \eta) = 345.44 \text{ mm}$$

$$L_{b,p}^F = L_{b,w}^F \eta + L_{b,f}^F (1 - \eta) = 123.77 \text{ mm}$$

The local buckling half-wavelength $L_{b,cs}$ of the full cross-section is then calculated as:

$$L_{b,cs} = L_{b,p}^{SS} - \xi(L_{b,p}^{SS} - L_{b,p}^F) = 345.44 - 0.165(345.44 - 123.77) = 308.96 \text{ mm}$$

Note that the full cross-section local buckling half-wavelength $L_{b,cs}$ determined using the finite strip analysis software CUFSM [21] is equal to 300.00 mm for the considered cross-section and loading type.

7.2.3. GMNIA using beam finite elements adopting the anisothermal approach

GMNIA is performed using 120 beam finite elements to discretise the beam over its 6179.26 mm length, indicating that each beam finite element has a length of 51.49 mm and 6 elements occur over the local buckling half-wavelength $L_{b,cs}$ of 308.96 mm. Since the member is fully laterally restrained and not subjected to axial compression, the modelling of the equivalent imperfections is not required. The analysis is completed by first increasing the mid-span load P to 69.18 kN followed by the application of an incrementally increasing temperature. The elevated temperature cross-section slenderness $\bar{\lambda}_{p,\theta}$ is calculated at each temperature increment as follows:

$$\bar{\lambda}_{p,\theta} = \sqrt{\frac{f_y}{\sigma_{cr,cs}}} \sqrt{\frac{k_{p0,2,\theta}}{k_{E,\theta}}}$$

where $k_{p0,2,\theta}$ is the 0.2% proof strength reduction factor and $k_{E,\theta}$ is the Young's modulus reduction factor. In addition, $\epsilon_{csm,\theta}$ is determined at

each temperature increment using the elevated temperature base curve shown in Fig. 2. The calculated elevated temperature cross-section slendernesses $\bar{\lambda}_{p,\theta}$ of the beam cross-section are less than 0.68 (i.e. $\bar{\lambda}_{p,\theta} < 0.68$); thus, the beam cross-section is considered non-slender and $\epsilon_{csm,\theta}/\epsilon_{y,\theta}$ is determined at each temperature increment as:

$$\epsilon_{csm,\theta}/\epsilon_{y,\theta} = \frac{0.25}{\bar{\lambda}_{p,\theta}^{-3.6}} + \frac{0.002}{\epsilon_{y,\theta}} \leq \left(\Omega, \frac{C_1}{\epsilon_{y,\theta}} \right)$$

where the upper limit Ω is set to 15 (i.e. $\Omega = 15$), the upper limit C_1 is equal to 0.02 (i.e. $C_1 = 0.02$) and $\epsilon_{y,\theta}$ is the elevated temperature yield strain calculated by dividing the elevated temperature 0.2% proof strength $f_{p0,2,\theta}$ by the elevated temperature Young's modulus E_θ (i.e. $\epsilon_{y,\theta} = f_{p0,2,\theta}/E_\theta$). The applied load P corresponds to a maximum design shear force V_{Ed} of 34.59 kN (i.e. $V_{Ed} = P/2 = 34.59$ kN). The shear resistance is calculated using EN 1993-1-2 [6] at each temperature increment as:

$$V_{fi,Rd} = A_v(k_{y,\theta} f_y / \sqrt{3}) / \gamma_{M,fi}$$

where $k_{y,\theta}$ is the elevated temperature yield strength reduction factor, A_v is the shear area calculated as $A - 2bt_f + (t_w + 2r)t_f$ for rolled I-sections subject to loading parallel to the web and $\gamma_{M,fi}$ is a partial factor at the fire limit state equal to 1.00. Since the maximum shear force V_{Ed} remains less than half of the shear capacity at elevated temperatures $V_{fi,Rd}$ (i.e. $V_{Ed} = 34.59$ kN $<$ $0.5V_{fi,Rd}$) throughout the analysis, the strain limit $\epsilon_{csm,\theta}$ does not need to be reduced to account for high shear stresses. The strain limit $\epsilon_{csm,\theta}$ calculated at each increment is then compared to the strains $\epsilon_{Ed,\theta}$ averaged over a length equal to the local buckling half-wavelength of the cross-section $L_{b,cs}$. Fig. 22 shows the development of the averaged strain $\epsilon_{Ed,\theta}$ at the critical cross-section versus the temperature. As can be seen in Fig. 22, the temperature θ_{csm} in the beam at which the averaged strain at the critical cross-section $\epsilon_{Ed,\theta}$ reaches the strain limit $\epsilon_{csm,\theta}$ of 0.0124 is equal to 599.66 °C. The critical temperature θ_{cr} of the beam based on the ISO 834-1 [44] and BS 476-20 [46] standards where the temperature at which the mid-span deflection is equivalent to $L/30 = 205.98$ mm corresponds to a temperature of 651.80 °C. Since the temperature at which the strain limit is reached θ_{csm} is less than the critical temperature θ_{cr} (i.e. $\theta_{csm} < \theta_{cr}$), the capacity of the steel beam is governed by the strain limit.

7.2.4. Resistance verification against applied load

The characteristic value of the resistance θ_{Rk} of the beam is equal to the temperature at which the critical averaged strain first reaches the strain limit θ_{csm} (i.e. $\theta_{Rk} = \theta_{csm}$). The design value of this resistance θ_{Rd} is calculated by dividing the temperature at which the strain limit is attained θ_{Rk} by the partial factor for resistance in fire conditions $\gamma_{M,fi}$ equal to 1.00 (i.e. $\gamma_{M,fi} = 1.00$), thus the design resistance is given by:

$$\theta_{Rd} = \frac{\theta_{Rk}}{\gamma_{M,fi}} = \frac{599.66}{1.00} = 599.66 \text{ °C}$$

Comparing the limit temperature θ_{Rd} to the design fire temperature θ_{Ed} of 550.00 °C:

$$\frac{\theta_{Rd}}{\theta_{Ed}} = \frac{599.66}{550.00} = 1.09 \geq 1.00 \quad \therefore \text{Pass}$$

Therefore, the beam is deemed satisfactory. Note that the design limit temperature θ_{Rd} determined using the benchmark shell finite element model is 646.77 °C. It is also of interest to note that when the isothermal analysis approach is adopted for the solution of the problem where the temperature of the member is first increased and then it is loaded up to failure, the ultimate failure load of 69.18 kN corresponds to the limit temperature θ_{Rd} equal to 603.06 °C which is very similar to the limit temperature θ_{Rd} of 599.66 °C obtained using the anisothermal analysis technique.

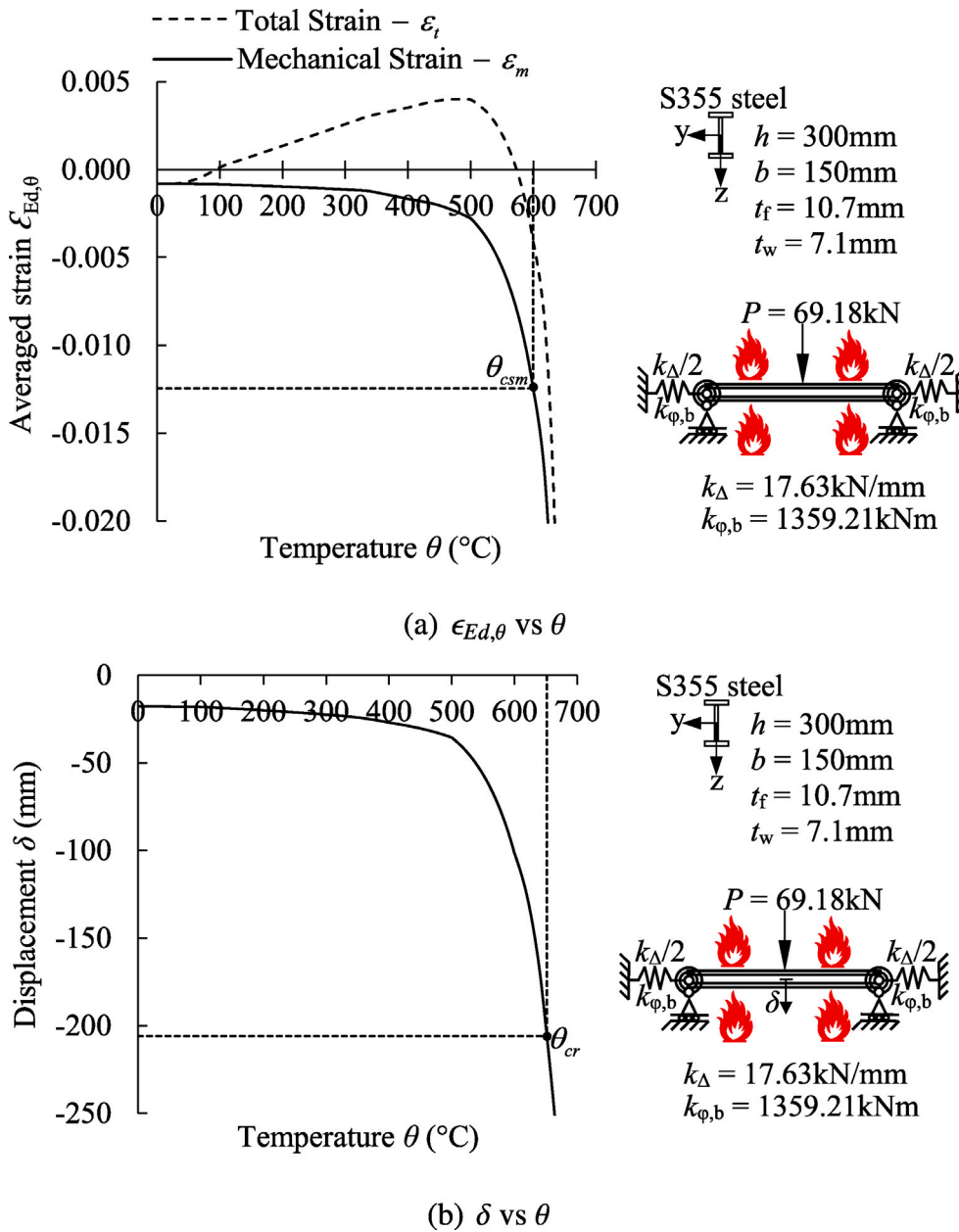


Fig. 22. Averaged strain at the critical cross-section and mid-span displacement plotted against temperature for the IPE 300 restrained beam derived by conducting anisothermal analysis.

8. Conclusions

An advanced structural steel fire design method performed through GMNIA with strain limits using beam finite elements is proposed and applied to the fire design of steel beams and beam-columns in this paper. Benchmark shell finite element models capable of replicating the behaviour of steel beams and beam-columns in fire were established and validated. The proposed fire design method was then extensively verified through parametric studies considering steel beams and beam-columns analysed using the isothermal analysis technique and axially unrestrained, axially restrained and axially and rotationally restrained beams and beam-columns analysed using the anisothermal analysis technique. The results from the parametric studies were also compared against the predictions from the European structural steel fire design standard EN 1993-1-2 [6]. It was observed that the proposed fire design approach provides consistent and safe-sided design predictions which are significantly more accurate and reliable than the design predictions

from EN 1993-1-2 [6]. The proposed method was previously verified for the fire design of steel columns [13]. Through this paper, the accuracy, safety and reliability of the method were demonstrated for steel beams and beam-columns as part of the establishment of a new, advanced structural steel fire design framework that effectively uses the current computational resources available to the structural engineering profession. Future research will further extend the proposed GMNIA with strain limits based structural steel fire design approach to the fire design of structural steel systems.

CRediT authorship contribution statement

Hasan Murtaza: Methodology, Software, Validation, Formal analysis, Investigation, Data curation, Writing – original draft, Visualization.
Merih Kucukler: Conceptualization, Methodology, Software, Investigation, Writing – original draft, Writing – review & editing, Supervision, Project administration, Funding acquisition.

Declaration of competing interest

The authors declare that there is no conflict of interest.

Data availability

Data will be made available on request.

References

- [1] Franssen JM, Gernay T. Modeling structures in fire with SAFIR®: Theoretical background and capabilities. *J Struct Fire Eng* 2017;8(3):300–23.
- [2] Possidente L, Tondini N, Battini JM. 3D beam element for the analysis of torsional problems of steel-structures in fire. *J Struct Eng, ASCE* 2020;146(7):04020125.
- [3] Jiang J, Usmani A. Modeling of steel frame structures in fire using OpenSees. *Comput Struct* 2013;118:90–9.
- [4] Saab HA, Nethercot DA. Modelling steel frame behaviour under fire conditions. *Eng Struct* 1991;13(4):371–82.
- [5] Landesmann A, Batista EM, Alves JLD. Implementation of advanced analysis method for steel-framed structures under fire conditions. *Fire Saf J* 2005;40(4):339–66.
- [6] EN 1993-1-2, Eurocode 3 Design of steel structures-Part 1-2: General rules – Structural Fire Design. Brussels: European Committee for Standardization (CEN); 2005.
- [7] prEN 1993-1-2, final draft of Eurocode 3 Design of steel structures-Part 1-2: General rules – Structural Fire Design. Brussels: European Committee for Standardization (CEN); 2019.
- [8] Couto C, Vila Real P, Lopes N, Zhao B. Effective width method to account for the local buckling of steel thin plates at elevated temperatures. *Thin-Walled Struct* 2014;84:134–49.
- [9] Couto C, Vila Real P, Lopes N, Zhao B. Resistance of steel cross-sections with local buckling at elevated temperatures. *J Constr Steel Res* 2015;109:101–14.
- [10] Maia É, Couto C, Vila Real P, Lopes N. Critical temperatures of class 4 cross-sections. *J Constr Steel Res* 2016;121:370–82.
- [11] Li L, Paquet J, Couto C, Vila Real P, Boissonnade N. Fire local stability of steel I-sections under simple load cases. *Eng Struct* 2023;283:115874.
- [12] Li L, Paquet J, Couto C, Vila Real P, Boissonnade N. Improved fire design of steel I-sections under combined compression and bending. *Structures* 2023;53:346–60.
- [13] Murtaza H, Kucukler M. Fire design of steel columns through second-order inelastic analysis with strain limits. *Thin-Walled Struct* 2023;184:110458.
- [14] Fieber A, Gardner L, Macorini L. Design of structural steel members by advanced inelastic analysis with strain limits. *Eng Struct* 2019;199:109624.
- [15] Fieber A, Gardner L, Macorini L. Structural steel design using second-order inelastic analysis with strain limits. *J Constr Steel Res* 2020;168:105980.
- [16] Quan C, Kucukler M, Gardner L. Design of web-tapered steel I-section members by second-order inelastic analysis with strain limits. *Eng Struct* 2020;224:111242.
- [17] Quan C, Kucukler M, Gardner L. Out-of-plane stability design of steel beams by second-order inelastic analysis with strain limits. *Thin-Walled Struct* 2021;169:108352.
- [18] Walport F, Gardner L, Nethercot DA. Design of structural stainless steel members by second order inelastic analysis with CSM strain limits. *Thin-Walled Struct* 2021;159:107267.
- [19] Walport F, Chan HU, Nethercot DA, Gardner L. Design of stainless steel structural systems by GMNIA with strain limits. *Eng Struct* 2023;276:115339.
- [20] Gardner L, Fieber A, Macorini L. Formulae for calculating elastic local buckling stresses of full structural cross-sections. *Structures* 2019;17:2–20.
- [21] Schafer BW, Adany S. Buckling analysis of cold-formed steel members using CUFSM: Conventional and constrained finite strip methods. In: Eighteenth international specialty conference on cold-formed steel structures, Orlando, FL. 2006, p. 39–54.
- [22] Theofanous M, Prospert T, Knobloch M, Gardner L. The continuous strength method for steel cross-section design at elevated temperatures. *Thin-Walled Struct* 2016;98:94–102.
- [23] Afshan S, Gardner L. The continuous strength method for structural stainless steel design. *Thin-Walled Struct* 2013;68:42–9.
- [24] Anwar-Us-Saadat M, Ashraf M, Ahmed S. Behaviour and design of stainless steel slender cross-sections subjected to combined loading. *Thin-Walled Struct* 2016;104:225–37.
- [25] Zhao O, Afshan S, Gardner L. Structural response and continuous strength method design of slender stainless steel cross-sections. *Eng Struct* 2017;140:14–25.
- [26] Yang K-C, Lee H-H, Chan O. Performance of steel H columns loaded under uniform temperature. *J Constr Steel Res* 2006;62(3):262–70.
- [27] Yang K-C, Hsu R. Structural behavior of centrally loaded steel columns at elevated temperature. *J Constr Steel Res* 2009;65(10–11):2062–8.
- [28] Yang K-C, Chen S-J, Lin C-C, Lee H-H. Experimental study on local buckling of fire-resisting steel columns under fire load. *J Constr Steel Res* 2005;61(4):553–65.
- [29] Pauli J, Somaini D, Knobloch M, Fontana M. Experiments on steel columns under fire conditions. IBK test report no. 340, ETH Zürich: Institute of Structural Engineering (IBK); 2012.
- [30] Feng M, Wang YC, Davies JM. Structural behaviour of cold-formed thin-walled short steel channel columns at elevated temperatures. Part 1: Experiments. *Thin-Walled Struct.* 2003;41(6):543–70.
- [31] Yang K-C, Lee H-H, Chan O. Experimental study of fire-resistant steel H-columns at elevated temperature. *J Constr Steel Res* 2006;62(6):544–53.
- [32] Wang W, Kodur V, Yang X, Li G. Experimental study on local buckling of axially compressed steel stub columns at elevated temperatures. *Thin-Walled Struct* 2014;82:33–45.
- [33] Yang KC, Yang FC. Fire performance of restrained welded steel box columns. *J Constr Steel Res* 2015;107:173–81.
- [34] Lan X, Li S, Zhao O. Local buckling of hot-rolled stainless steel channel section stub columns after exposure to fire. *J Constr Steel Res* 2021;187:106950.
- [35] Su A, Jiang K, Wang Y, Zhao O. Experimental and numerical investigations into S960 ultra-high strength steel welded I-section stub columns after exposure to elevated temperatures. *Thin-Walled Struct* 2023;183:110349.
- [36] Sharhan A, Wang W, Li X, Al-azzani H. Steady and transient state tests on local buckling of high strength Q690 steel stub columns. *Thin-Walled Struct* 2021;167:108214.
- [37] Walport F, Gardner L, Nethercot DA. Equivalent bow imperfections for use in design by second order inelastic analysis. *Structures* 2020;26:670–85.
- [38] EN 1090-2, Execution of steel structures and aluminium structures-Part 2: Technical requirements for steel structures. Brussels: European Committee for Standardization (CEN); 2008.
- [39] Fieber A, Gardner L, Macorini L. Formulae for determining elastic local buckling half-wavelengths of structural steel cross-sections. *J Constr Steel Res* 2019;159:493–506.
- [40] EN 1993-1-1, Eurocode 3 Design of steel structures-Part 1-1: General rules and rules for buildings. Brussels: European Committee for Standardization (CEN).
- [41] Abaqus 2018 reference manual. Simulia, Dassault Systemes; 2018.
- [42] ANSYS 18 user manual. PA: ANSYS Inc Canonsburg; 2018.
- [43] Franssen JM. User's manual for SAFIR 2011. A computer program for analysis of structures subjected to fire. Belgium: University of Liege; 2011.
- [44] ISO 834-1 Fire-resistance tests – Elements of building construction – Part 1: General requirements. Geneva: International Organization for Standardization (ISO); 2020.
- [45] Dwaikat MMS, Kodur V. A performance based methodology for fire design of restrained steel beams. *J Constr Steel Res* 2011;67(3):510–24.
- [46] BS 476-20 Fire tests on building materials and structures – Part 20: Method for determination of the fire resistance of elements of construction (general principles). London: The British Standards Institution (BSI); 2014.
- [47] Segura G, Pournaghshband A, Afshan S, Mirambell E. Numerical simulation and analysis of stainless steel frames at high temperature. *Eng Struct* 2021;227:111446.
- [48] Shen Y, Chacón R. Flexural stiffness reduction for stainless steel SHS and RHS members prone to local buckling. *Thin-Walled Struct* 2020;155:106939.
- [49] Ding R, Fan S, Chen G, Li C, Du E, Liu C. Fire resistance design method for restrained stainless steel H-section columns under axial compression. *Fire Saf J* 2019;108:102837.
- [50] Maraveas C, Gernay T, Franssen J-M. An equivalent stress method to account for local buckling in beam finite elements subjected to fire. *J Struct Fire Eng* 2019;10(3):340–53.
- [51] Maraveas C, Gernay T, Franssen JM. Sensitivity of elevated temperature load carrying capacity of thin-walled steel members to local imperfections. *Appl Fire Eng* 2017;19–29.
- [52] ECCS, Ultimate limit state calculation of sway frames with rigid joints. Tech. Rep., No. 33, Technical Committee 8 (TC 8) of European Convention for Constructional Steelwork (ECCS); 1984.
- [53] Segura G, Arrayago I, Mirambell E. Plastic redistribution capacity of stainless steel frames in fire. *J Constr Steel Res* 2023;208:108019.
- [54] Kucukler M, Xing Z, Gardner L. Behaviour and design of stainless steel I-section columns in fire. *J Constr Steel Res* 2020;165:105890.
- [55] Kucukler M. Lateral instability of steel beams in fire: Behaviour, numerical modelling and design. *J Constr Steel Res* 2020;170:106095.
- [56] Kucukler M. Local stability of normal and high strength steel plates at elevated temperatures. *Eng Struct* 2021;243:112528.
- [57] Kucukler M. Shear resistance and design of stainless steel plate girders in fire. *Eng Struct* 2023;276:115331.
- [58] Quan C, Kucukler M. Cross-section resistance and design of stainless steel CHS and EHS at elevated temperatures. *Eng Struct* 2023;285:115996.
- [59] Quan C, Kucukler M. Simulation and cross-section resistance of stainless steel SHS and RHS at elevated temperatures. *Thin-Walled Struct* 2023;189:110849.
- [60] Dharma RB, Tan K-H. Rotational capacity of steel I-beams under fire conditions Part I: Experimental study. *Eng Struct* 2007;29(9):2391–402.
- [61] Liu TCH, Fahad MK, Davies JM. Experimental investigation of behaviour of axially restrained steel beams in fire. *J Constr Steel Res* 2002;58(9):1211–30.
- [62] Couto C, Vila Real P, Lopes N, Zhao B. Numerical investigation of the lateral-torsional buckling of beams with slender cross sections for the case of fire. *Eng Struct* 2016;106:410–21.

- [63] Couto C, Coderre T, Vila Real P, Boissonnade N. Cross-section capacity of RHS and SHS at elevated temperatures: Comparison of design methodologies. *Structures* 2021;34:198–214.
- [64] Arrais F, Lopes N, Real PV. Fire design of stainless steel columns with hollow circular and elliptical sections. *J Constr Steel Res* 2023;210:108085.
- [65] Fang H, Chan T-M. Axial compressive strength of welded S460 steel columns at elevated temperatures. *Thin-Walled Struct* 2018;129:213–24.
- [66] Fang H, Chan T-M. Resistance of axially loaded hot-finished S460 and S690 steel square hollow stub columns at elevated temperatures. *Structures* 2019;17:66–73.
- [67] Fang H, Chan T-M. Behaviour and design of cold-formed normal-and high-strength steel SHS and RHS columns at elevated temperatures. *Thin-Walled Struct* 2022;180:109947.
- [68] Martinez J, Jeffers AE. Analysis of restrained composite beams exposed to fire. *Eng Struct* 2021;234:111740.
- [69] Kodur VKR, Dwaikat M. Effect of high temperature creep on the fire response of restrained steel beams. *Mater Struct* 2010;43(10):1327–41.
- [70] Franssen J-M. Failure temperature of a system comprising a restrained column submitted to fire. *Fire Saf J* 2000;34(2):191–207.
- [71] Kruppa J. Eurocodes–fire parts, proposal for a methodology to check the accuracy of assessment methods. *GEN TC*, 250, 1999.